# Molecular Interactions and Thermal Transport of Ionic Liquids with Carbon Nanomaterials – Supplementary Information

João M.P. França[a,b], Carlos A. Nieto de Castro[b], Agílio A.H. Pádua[a,*]

[a] Institut de Chimie de Clermont-Ferrand, Université Clermont Auvergne & CNRS, 63178 Aubière, France. *Email : agilio.padua@uca.fr

[b] Centro de Química Estrutural, Faculdade de Ciências, Universidade de Lisboa, Campo Grande, 1749-016, Lisboa, Portugal.

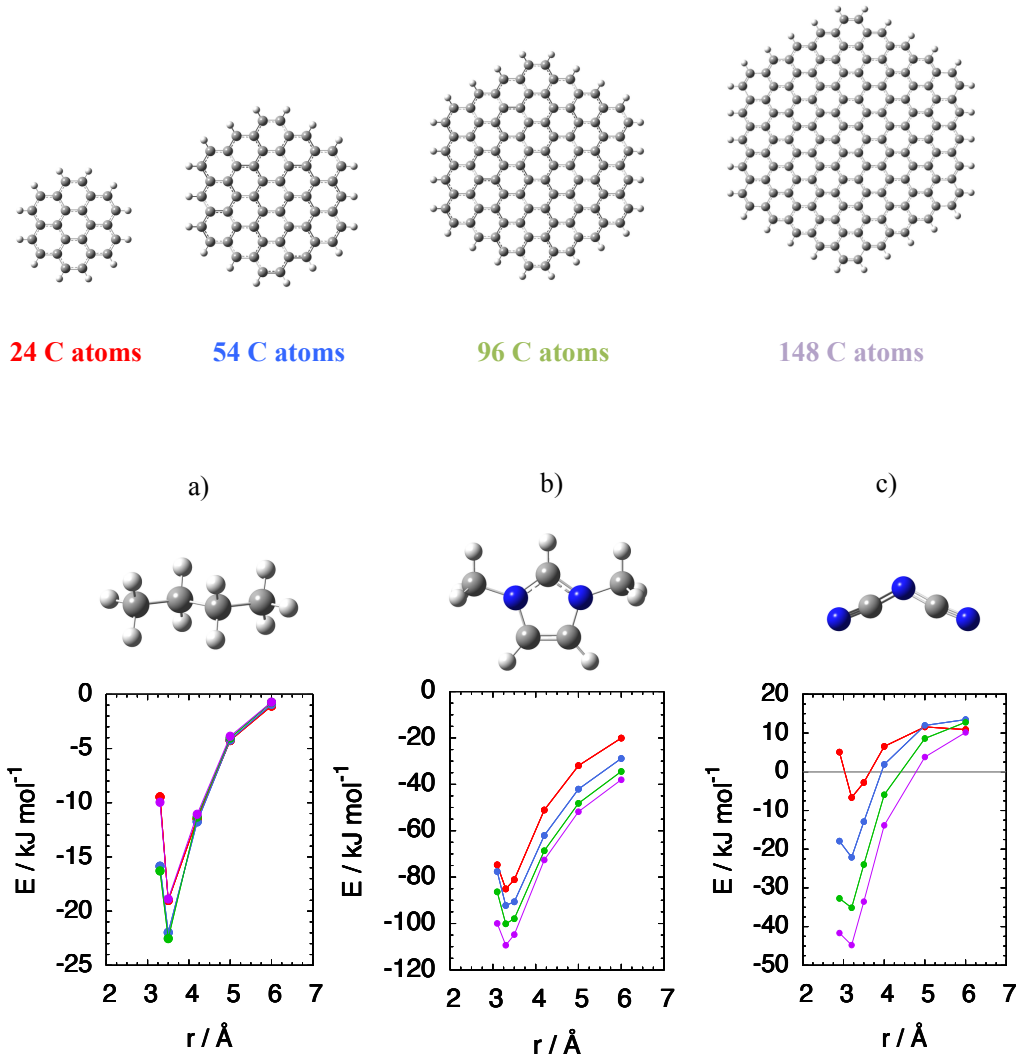


Figure S1. Evaluation of the effect of the size of the graphene flake on the potential energy of interaction with fragments of the ionic liquid, placed centered above the plane : a) butane, b) dimethylimidazolium cation, and c) dicyanamide anion.; red – 24 C atoms, blue – 54 C atoms, green – 96 C atoms; purple – 148 C atoms. Calculations performed using the density functional and basis set M06-2X/cc-pVTZ(-f), including corrections for basis set superposition error.

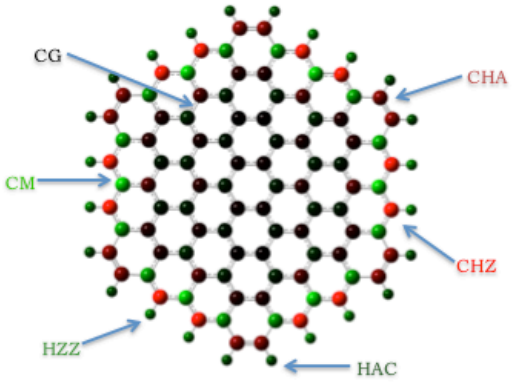


Figure S2. Partial charge scheme for a graphenic flake (δmax =0.05e).

Table S1. Values of the detailed partial charge scheme for graphene flakes.

| **Atom** | HAC | HZZ | CHA | CHZ | CM | CG |
|---|---|---|---|---|---|---|
| **q/e** | +0.09 | +0.16 | -0.18 | -0.34 | +0.18 | 0.00 |

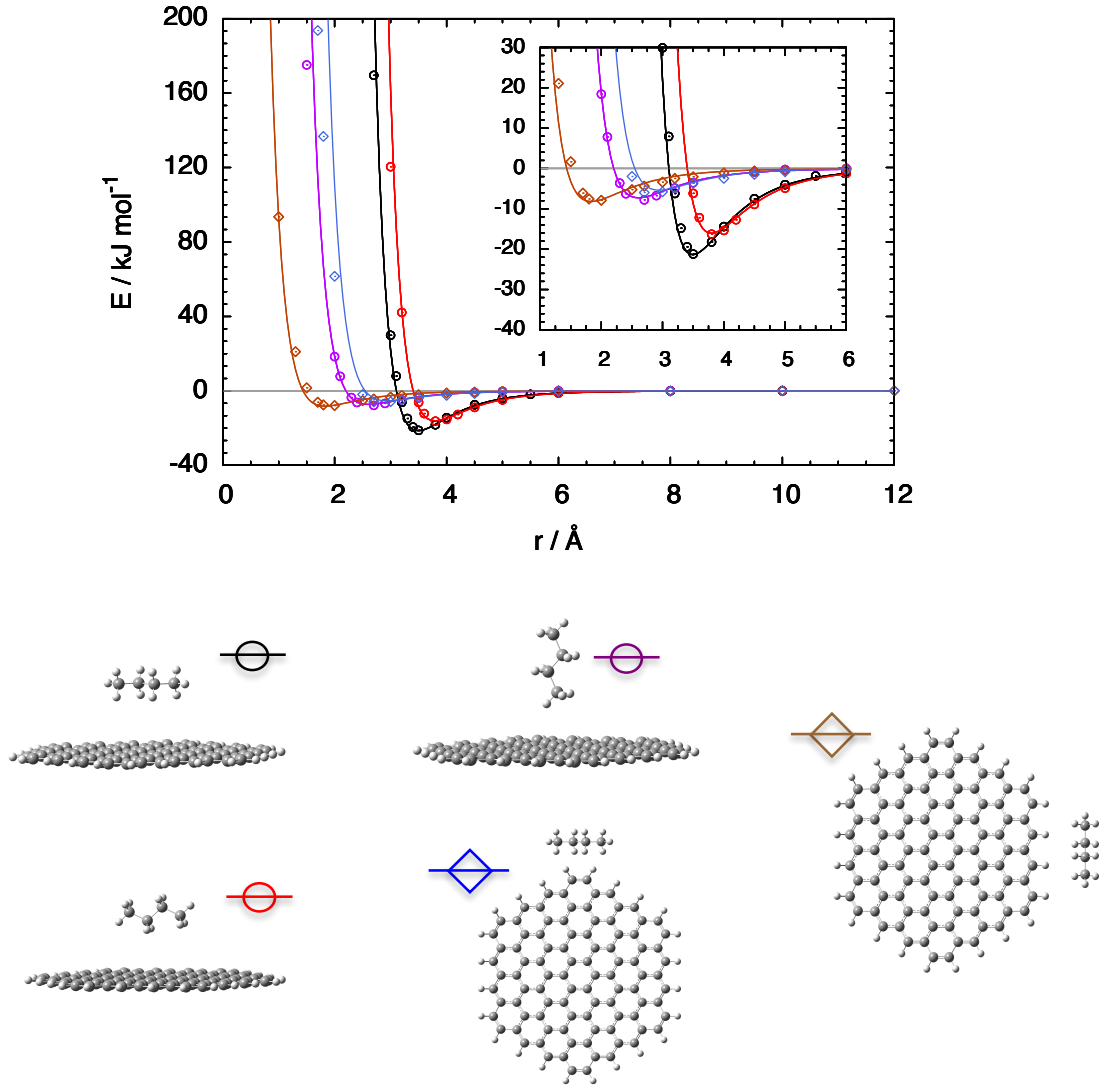


Figure S3. Potential energy of interaction between the **butane** fragment and a 96 C atom graphene flake. Symbols are quantum calculations at the M06-2X/cc-pVTZ level. Lines result from fitting the site-site *n-m* potential function. The color and the symbol below the plot indicate the orientation of the ionic liquid fragment regarding the graphene flake.

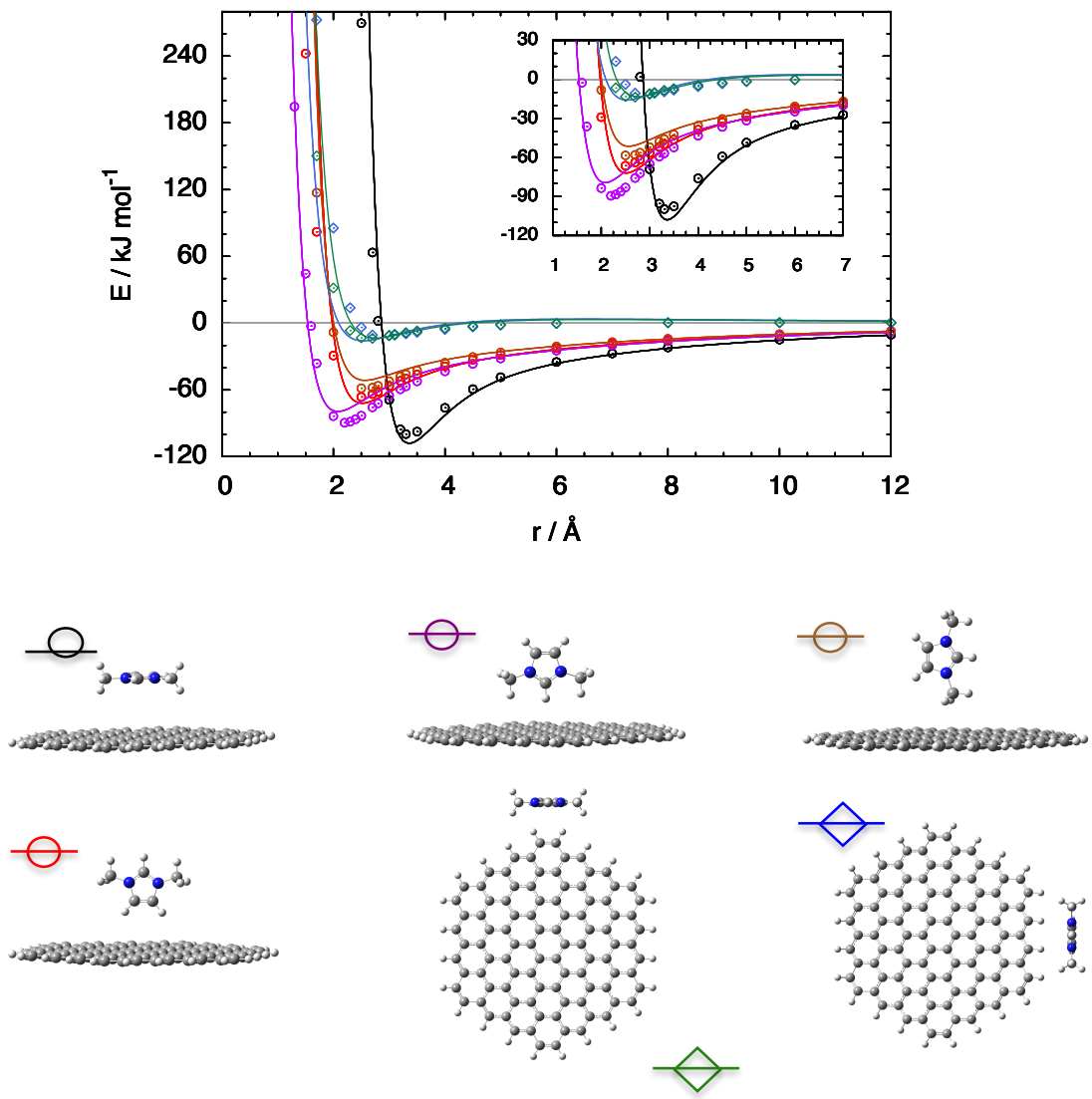


Figure S4. Potential energy of interaction between the **dimethylimidazolium** fragment and a 96 C atom graphene flake. Symbols are quantum calculations at the M06-2X/cc-pVTZ level. Lines result from fitting the site-site *n-m* potential function. The color and the symbol below the plot indicate the orientation of the ionic liquid fragment regarding the graphene flake.

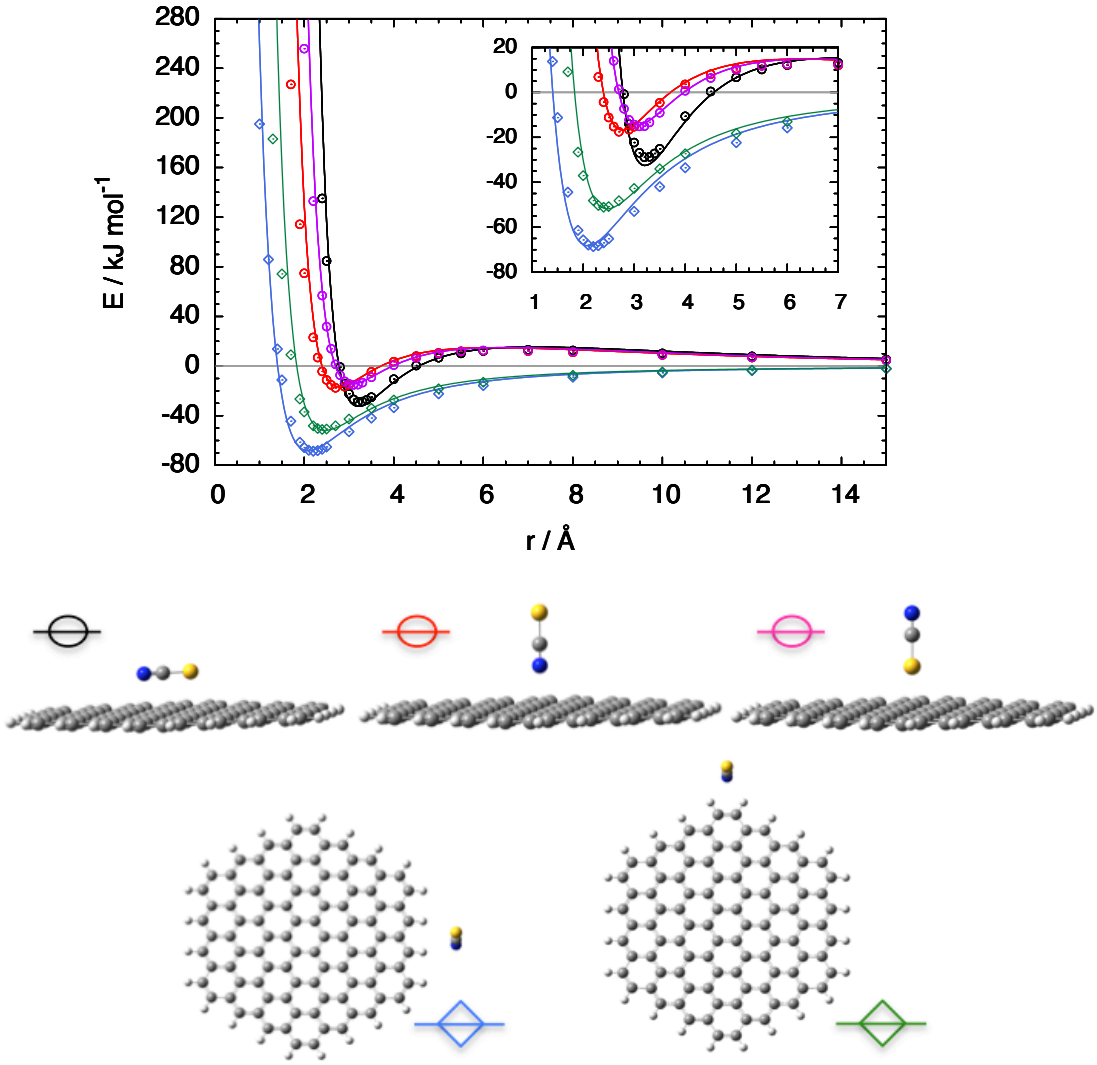


Figure S5. Potential energy of interaction between the **thiocyanate** fragment and a 96 C atom graphene flake. Symbols are quantum calculations at the M06-2X/cc-pVTZ level. Lines result from fitting the site-site *n-m* potential function. The color and the symbol below the plot indicate the orientation of the ionic liquid fragment regarding the graphene flake.

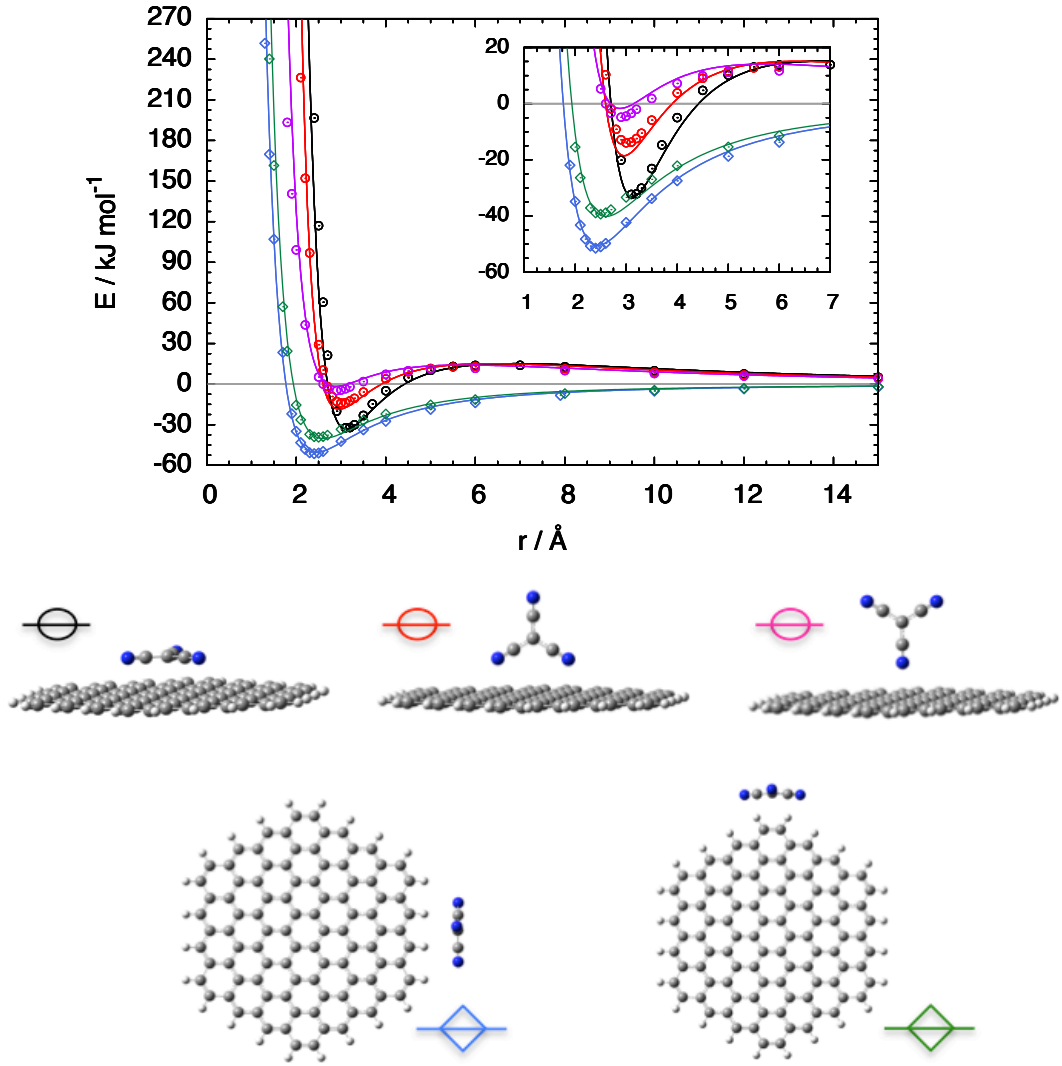


Figure S6. Potential energy of interaction between the **tricyanomethanide** fragment and a 96 C atom graphene flake. Symbols are quantum calculations at the M06-2X/cc-pVTZ level. Lines result from fitting the site-site *n-m* potential function. The color and the symbol below the plot indicate the orientation of the ionic liquid fragment regarding the graphene flake.

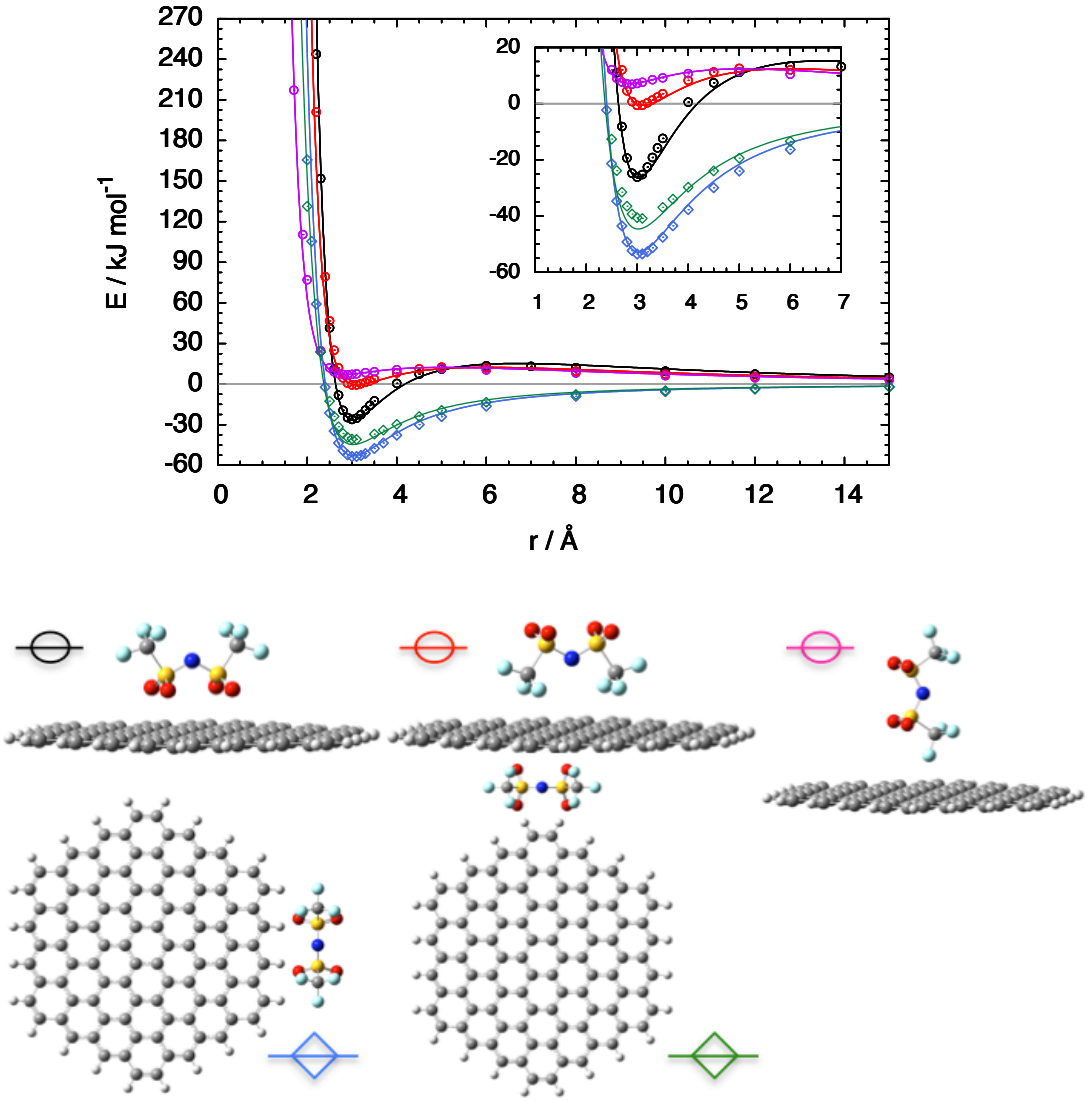


Figure S7. Potential energy of interaction between the **bis(trifluoromethylsulfonyl)imide** fragment and a 96 C atom graphene flake. Symbols are quantum calculations at the M06-2X/cc-pVTZ level. Lines result from fitting the site-site *n-m* potential function. The color and the symbol below the plot indicate the orientation of the ionic liquid fragment regarding the graphene flake.

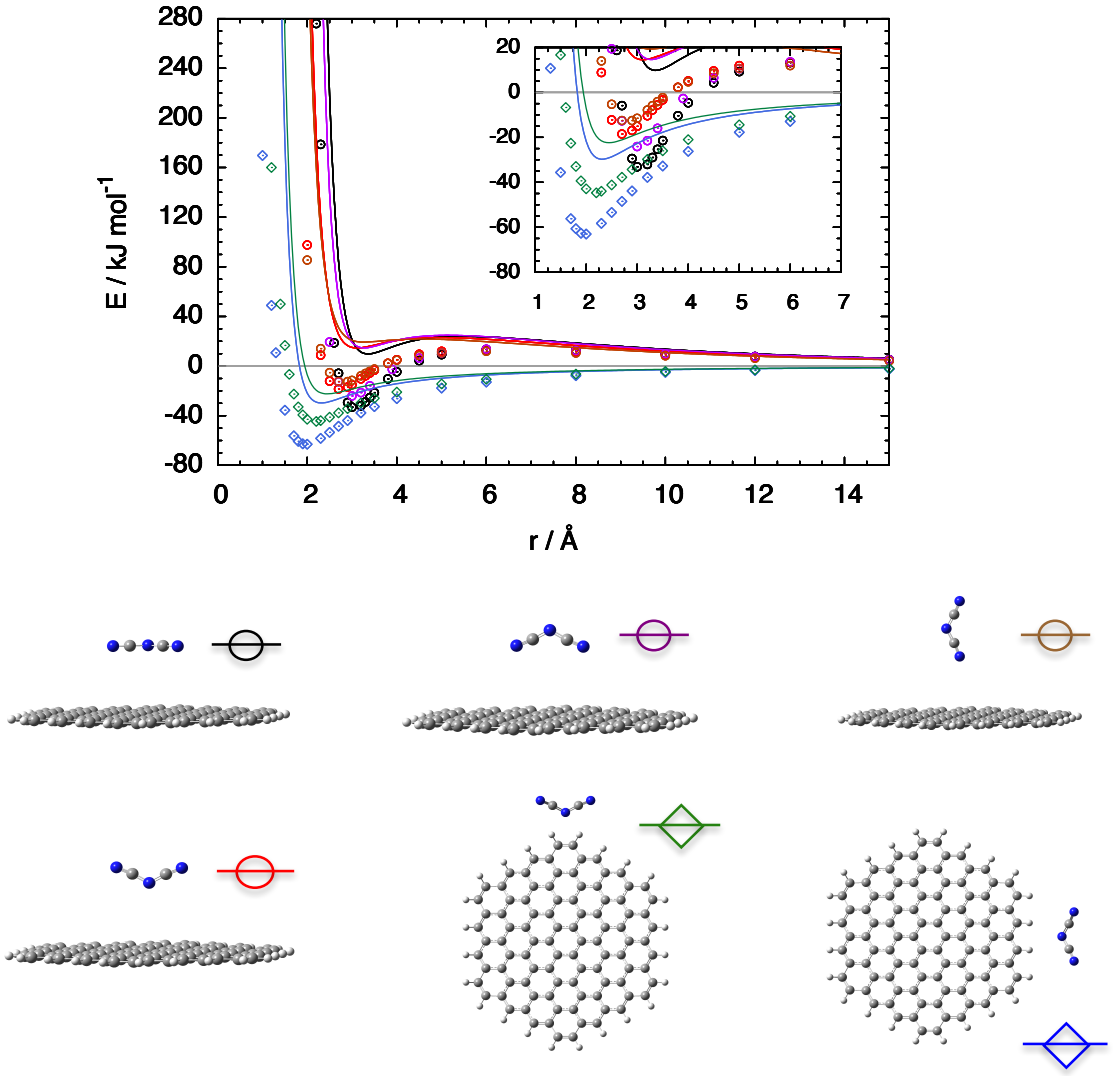


Figure S8. Potential energy of interaction between the **dicyanamide** fragment and a 96 C atom graphene flake. Symbols are quantum calculations at M06-2X/cc-pVTZ level. Lines are calculations using the **Lennard-Jones (12-6)** potential function with parameters from combining rules between LJ parameters of the dicyanamide anion and the force field for graphene.

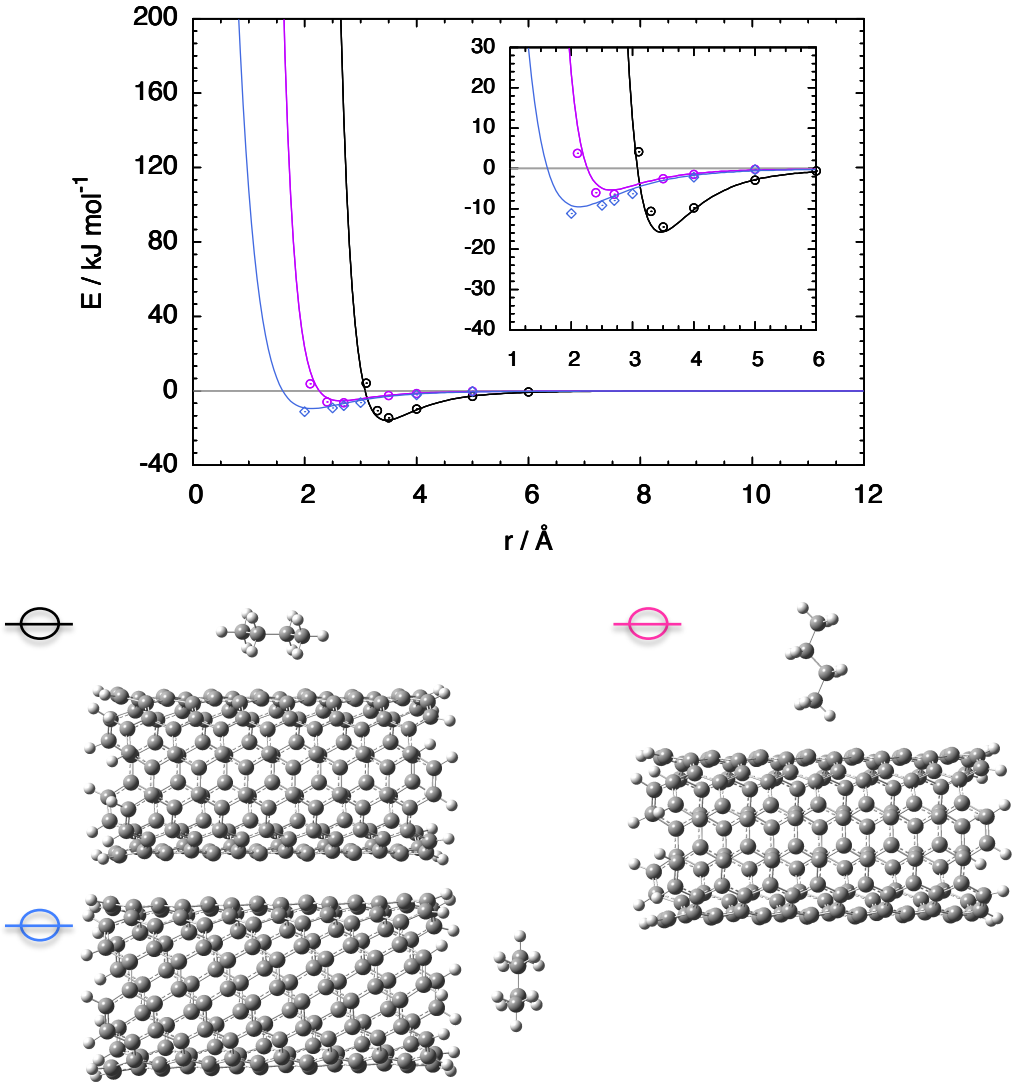


Figure S9. Potential energy of interaction between the **butane** fragment and a 168 C atom SWNT. Symbols are quantum calculations at the M06-2X/cc-pVTZ level. Lines are obtained from the *n-m* site-site potential functions using parameters derived from the fit to graphenic flakes.

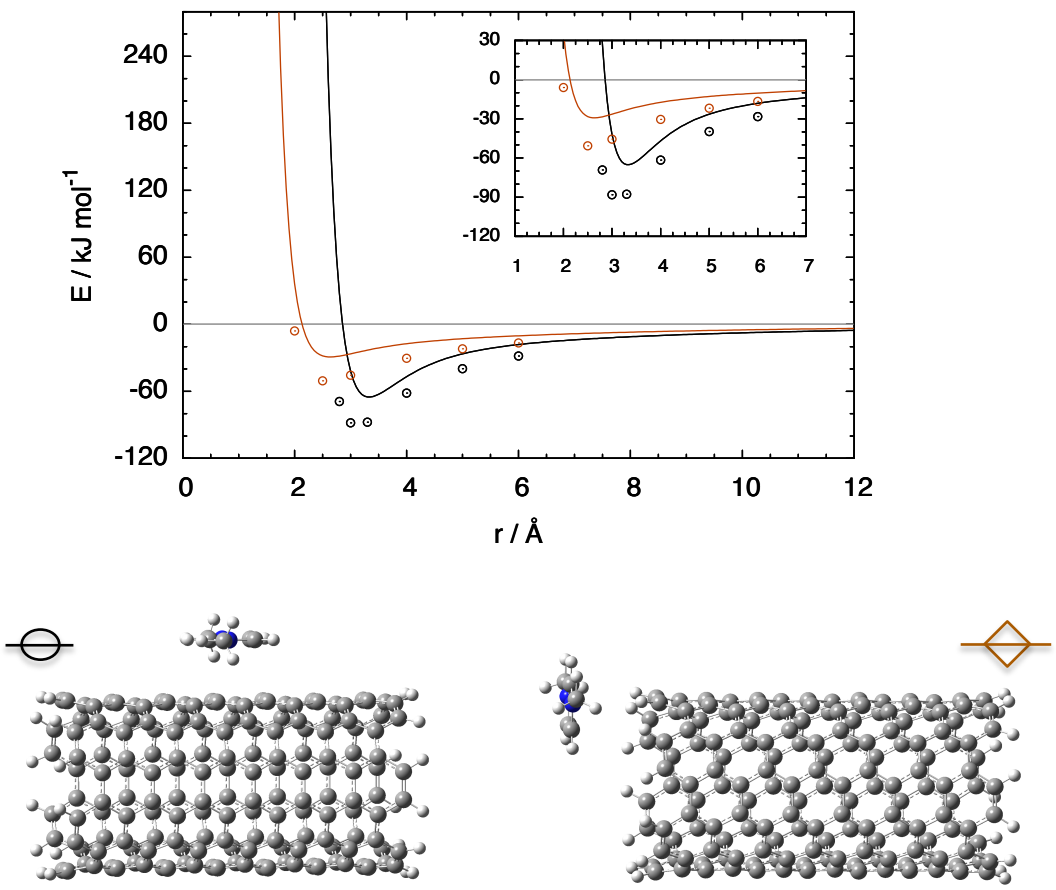


Figure S10. Potential energy of interaction between the **dimethylimidazolium** fragment and a 168 C atom SWNT. Symbols are quantum calculations at the M06-2X/cc-pVTZ level. Lines are obtained from the *n-m* site-site potential functions using parameters derived from the fit to graphenic flakes.

Table S2. Number of ion pairs used in molecular dynamics for each ionic liquid. Density values are at $T$ = 363K.

| Ionic liquid | $\rho$ (kg m$^{-3}$) | Ion pairs | |
|---|---|---|---|
| | | graphene | (7,7) & (10,10) |
| $[C_4C_1im][N(CN)_2]$ | 1020.6[a] | 388 | 950 |
| $[C_4C_1im][SCN]$ | 1031.73[b] | 401 | 960 |
| $[C_4C_1im][C(CN)_3]$ | 1004.6[c] | 336 | 800 |
| $[C_4C_1im][tf_2N]$ | 1375.58[d] | 252 | 600 |

a - J.M.P. França *et al., J. Chem. Thermodynamics* 79 (2014) 248–257
b- G. Vakili-Nezhaad *et al., J. Chem. Thermodynamics* 54 (2012) 148–154
c- P.J. Carvalho *et al., J. Chem. Eng. Data* **2010,** *55,* 645–652
d- C.A. Nieto de Castro, *et al., Fluid Phase Equilibria* 294 (2010) 157–179

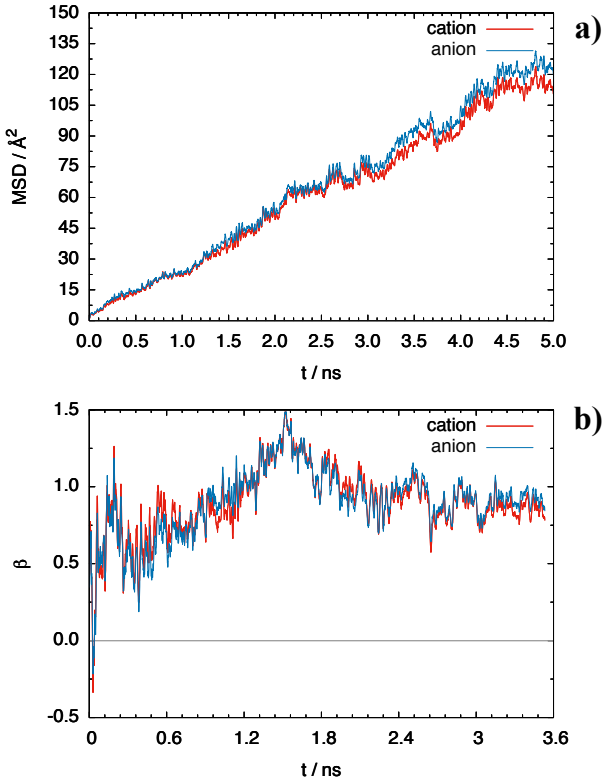


Figure S11. a) Global (xyz) mean-square displacement (MSD) and b) linearity parameter $\beta$ for the ions in the pure ionic liquid $[C_4C_1im][SCN]$ at 363K.

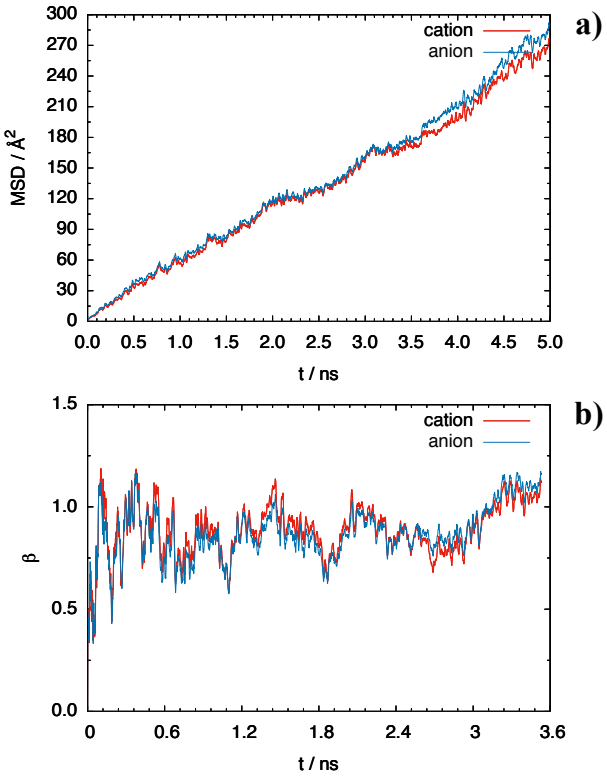


Figure S12. a) Global (xyz) mean-square displacement (MSD) and b) linearity parameter $\beta$ for the ions in the pure ionic liquid $[C_4C_1im][N(CN)_2]$ at 363K.

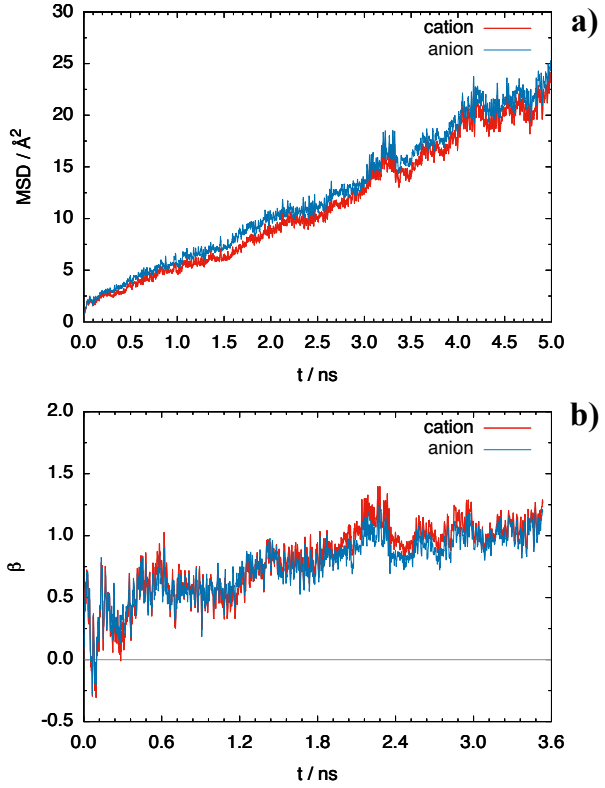


Figure S13. a) Global (xyz) mean-square displacement (MSD) and b) linearity parameter $\beta$ for the ions in the pure ionic liquid $[C_4C_1im][C(CN)_3]$ at 363K.

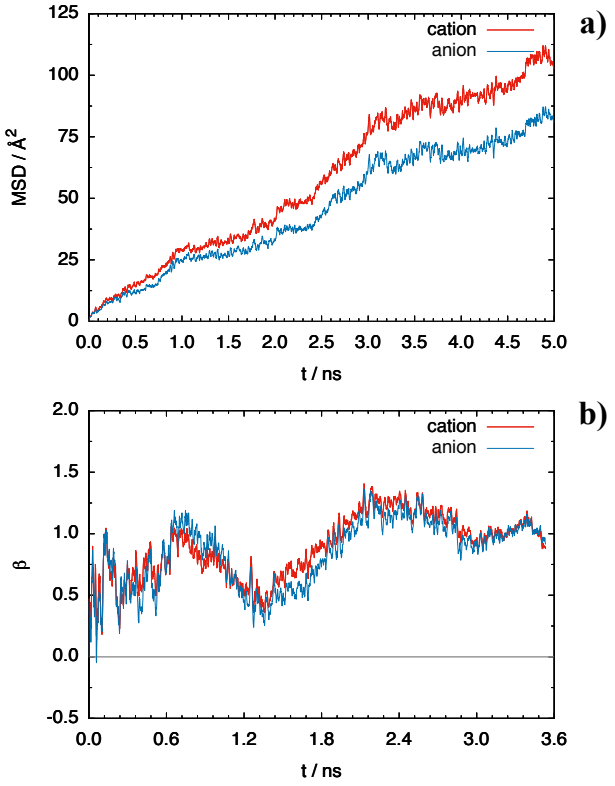


Figure S14. a) Global (xyz) mean-square displacement (MSD) and b) linearity parameter $\beta$ for the ions in the pure ionic liquid $[C_4C_1im][tf_2N]$ at 363K.

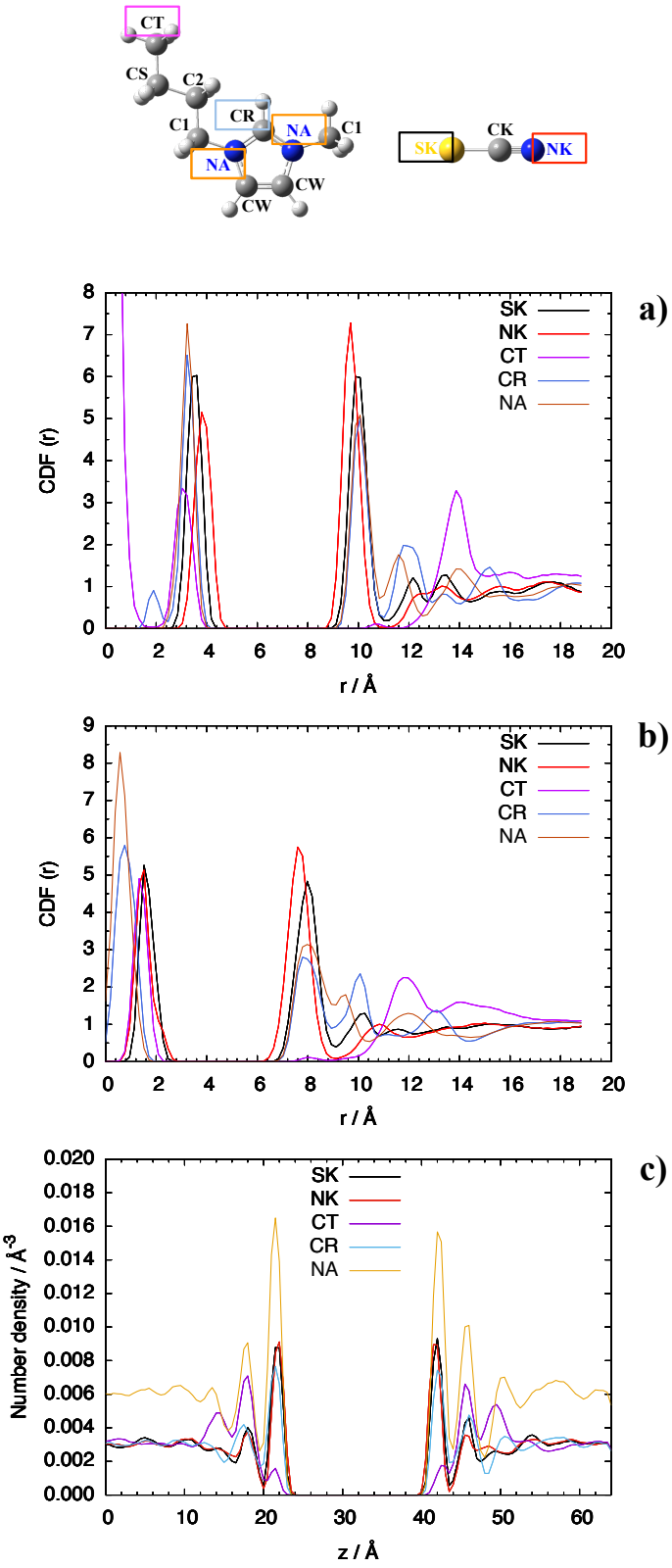


Figure S15. Cylindrical distribution function (CDF) of a) $[C_4C_1im][SCN]$ and SWNCT (10,10), b) $[C_4C_1im][SCN]$ and SWNCT (7,7) and c) Number density of $[C_4C_1im][SCN]$ and graphene. $T = 363$ K.

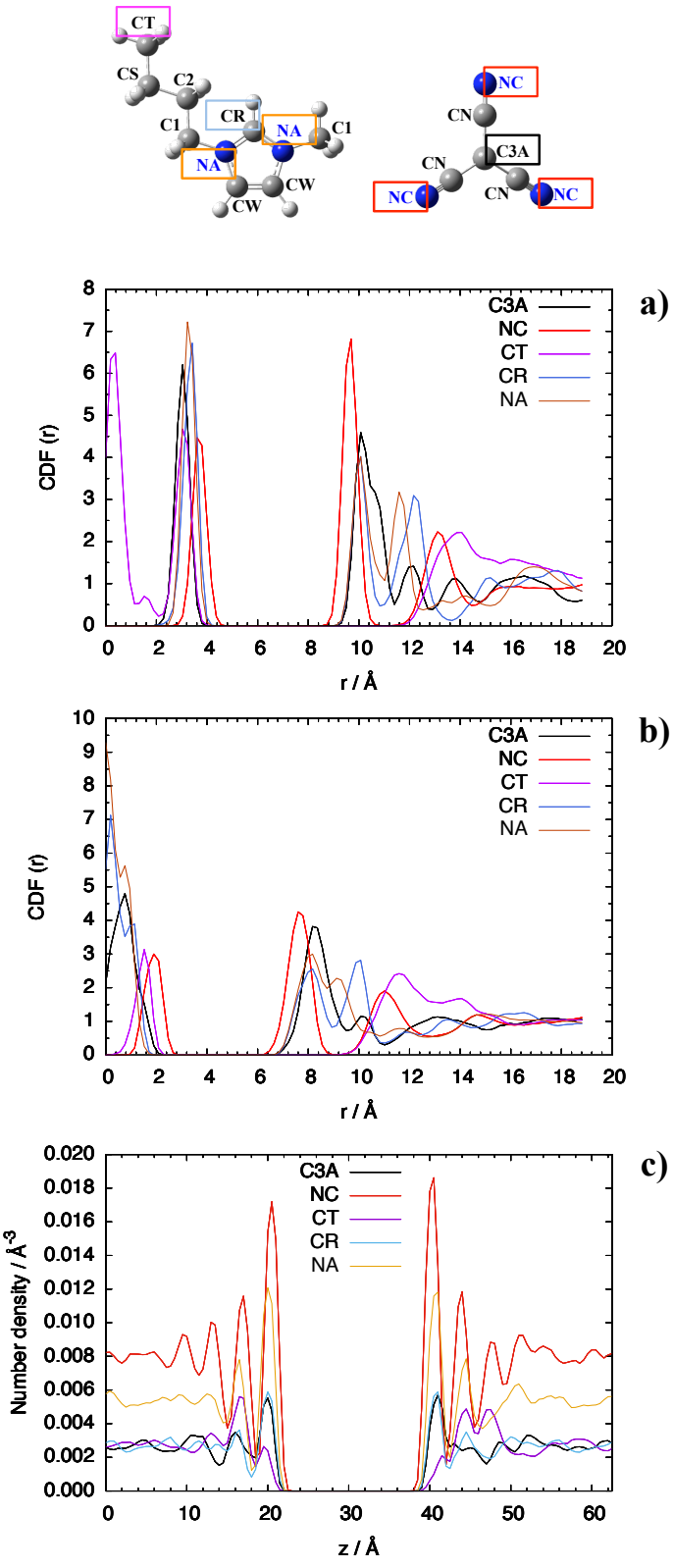


Figure S16. Cylindrical distribution function (CDF) of a) $[C_4C_1im][C(CN)_3]$ and SWNCT (10,10), b) $[C_4C_1im][C(CN)_3]$ and SWNCT (7,7) and c) Number density of $[C_4C_1im][C(CN)_3]$ and graphene. $T$ = 363 K.

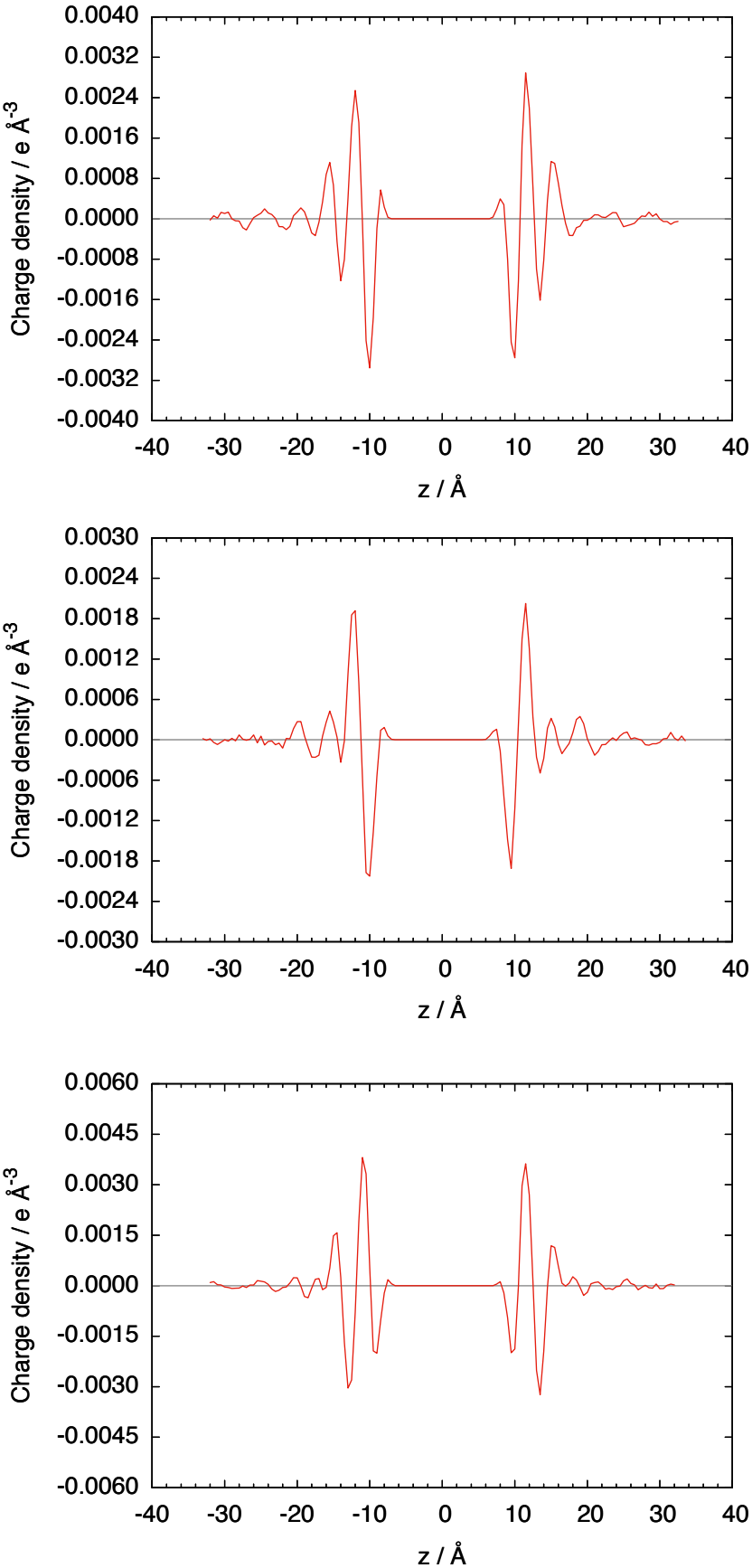


Figure S17. Electrostatic charge density profile of $[C_4C_1im][SCN]$ (top), $[C_4C_1im][N(CN)_2]$ (center) and $[C_4C_1im][tf_2N]$ (bottom) with graphene at $T$ = 423 K. The higher temperature was chosen in order to obtain better-converged profiles.

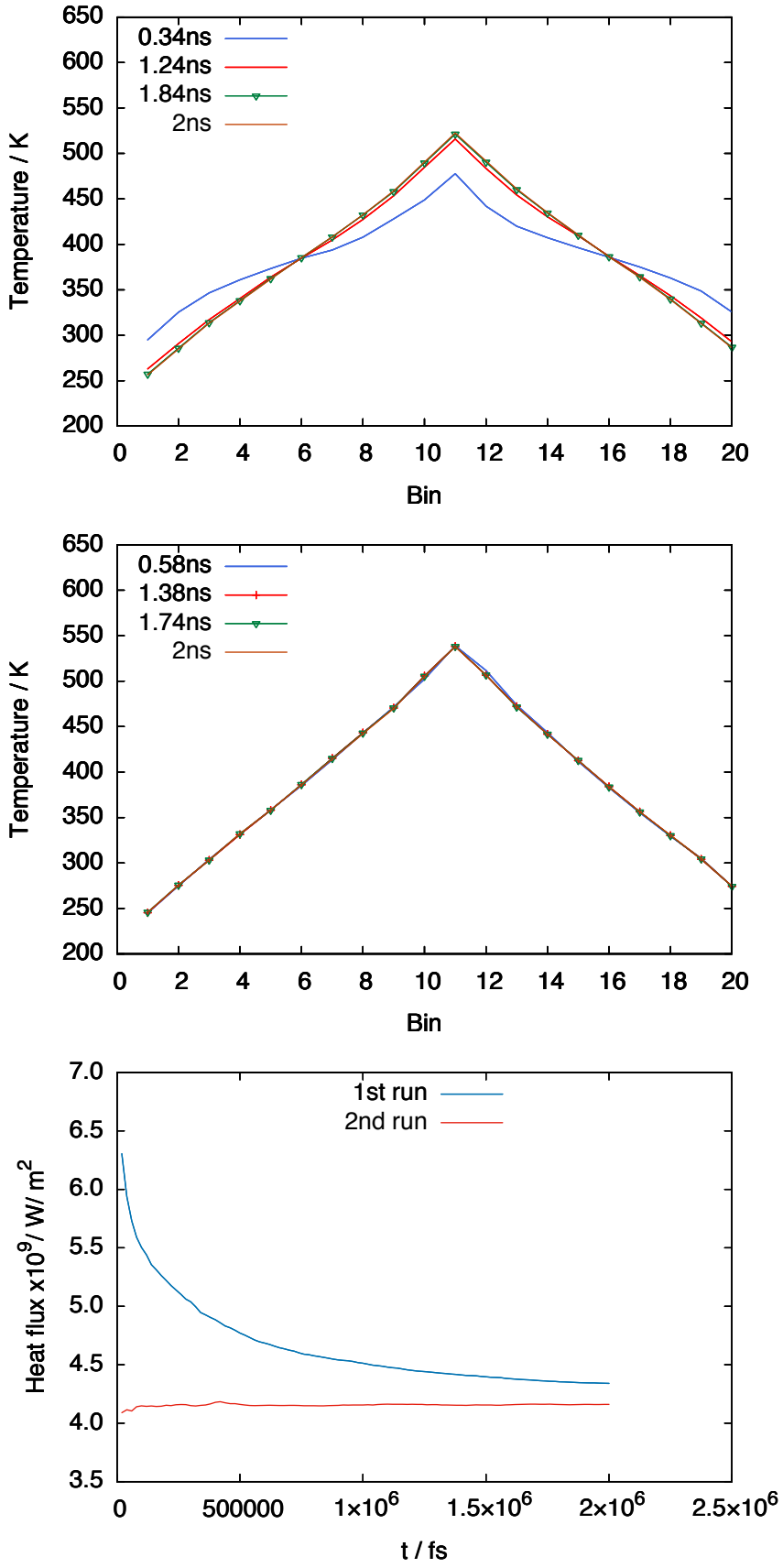


Figure S18 - Temperature profile along the simulation box (here represented in bins) during the first run (top), second run (middle) and heat flux (bottom) for pure $[C_4C_1im][tf_2N]$. These are referred to a 500 time steps exchange rate of kinetic energy at 383K.

Table S3. Thermal conductivities obtained from NEMD for pure IL, IL+SWCNT and IL+Graphene. “MP 350” stands for the Müller-Plathe method with a kinetic energy exchange rate of 350 time steps, while “MP 500” stands for a kinetic energy exchange rate of 500 time steps.

| T / K | $[C_4C_1im][tf_2N]$ | $[C_4C_1im][SCN]$ | $[C_4C_1im][N(CN)_2]$ | $[C_4C_1im][C(CN)_3]$ |
|---|---|---|---|---|
| | | $\lambda$ / W $K^{-1}m^{-1}$ IL MP 350 | | |
| 363 | 0.165 | 0.244 | 0.253 | 0.308 |
| 383 | 0.159 | 0.241 | 0.252 | 0.305 |
| 423 | 0.155 | 0.233 | 0.243 | 0.302 |
| | | $\lambda$ / W $K^{-1}m^{-1}$ IL MP 500 | | |
| 363 | 0.166 | 0.243 | 0.255 | 0.304 |
| 383 | 0.158 | 0.239 | 0.249 | 0.309 |
| 423 | 0.155 | 0.235 | 0.244 | 0.302 |
| | | $\lambda$ / W $K^{-1}m^{-1}$ IL + SWCNT MP 350 | | |
| 363 | 0.209 | 0.302 | 0.312 | 0.354 |
| 383 | 0.205 | 0.297 | 0.312 | 0.361 |
| 423 | 0.209 | 0.290 | 0.303 | 0.361 |
| | | $\lambda$ / W $K^{-1}m^{-1}$ IL + SWCNT MP 500 | | |
| 363 | 0.209 | 0.290 | 0.312 | 0.365 |
| 383 | 0.206 | 0.296 | 0.315 | 0.354 |
| 423 | 0.204 | 0.285 | 0.307 | 0.372 |
| | | $\lambda$ / W $K^{-1}m^{-1}$ IL + Graphene MP 350 | | |
| 363 | 0.066 | 0.109 | 0.127 | 0.130 |
| 383 | 0.068 | 0.117 | 0.122 | 0.135 |
| 423 | 0.069 | 0.116 | 0.121 | 0.138 |
| | | $\lambda$ / W $K^{-1}m^{-1}$ IL + Graphene MP 500 | | |
| 363 | 0.068 | 0.112 | 0.128 | 0.134 |
| 383 | 0.070 | 0.111 | 0.121 | 0.140 |
| 423 | 0.071 | 0.119 | 0.122 | 0.148 |
| | | $\lambda$ / W $K^{-1}m^{-1}$ IL MP 350 (bulk liquid from IL+Graphene) | | |
| 363 | 0.075 | 0.131 | 0.143 | 0.164 |
| 383 | 0.079 | 0.133 | 0.145 | 0.157 |
| 423 | 0.080 | 0.141 | 0.143 | 0.178 |
| | | $\lambda$ / W $K^{-1}m^{-1}$ IL MP 500 (bulk liquid from IL+Graphene) | | |
| 363 | 0.077 | 0.127 | 0.148 | 0.159 |
| 383 | 0.081 | 0.129 | 0.142 | 0.171 |
| 423 | 0.081 | 0.142 | 0.144 | 0.176 |

Table S4. Interfacial thermal conductivities obtained from NEMD for IL+Graphene. "MP 350" stands for the Müller-Plathe method with a kinetic energy exchange rate of 350 time steps, while "MP 500" stands for a kinetic energy exchange rate of 500 time steps.

| T / K | $[C_4C_1im][tf_2N]$ | $[C_4C_1im][SCN]$ | $[C_4C_1im][N(CN)_2]$ | $[C_4C_1im][C(CN)_3]$ |
|---|---|---|---|---|
| | $\lambda$ / W $K^{-1}m^{-1}$ IL + Graphene MP 350 | | | |
| 363 | 0.089 | 0.158 | 0.188 | 0.184 |
| 383 | 0.091 | 0.181 | 0.179 | 0.195 |
| 423 | 0.092 | 0.166 | 0.176 | 0.193 |
| | $\lambda$ / W $K^{-1}m^{-1}$ IL + Graphene MP 500 | | | |
| 363 | 0.090 | 0.166 | 0.184 | 0.197 |
| 383 | 0.094 | 0.176 | 0.176 | 0.201 |
| 423 | 0.094 | 0.176 | 0.179 | 0.217 |

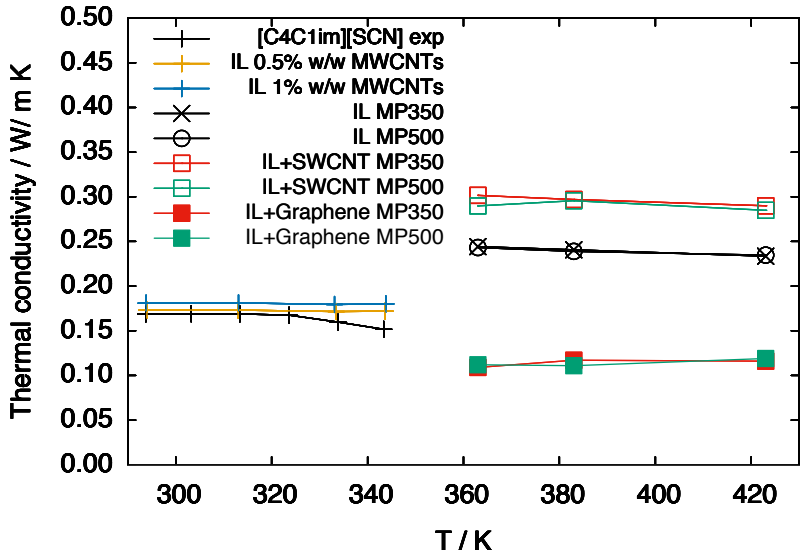


Figure S19. Thermal conductivity of $[C_4C_1im][SCN]$, pure and with carbon nanomaterials. Experimental results [J.M.P. França, S.M.S. Murshed, A.A.H Pádua, C.A. Nieto de Castro, "Thermal conductivity of Cyano and Phosphonium Ionic Liquids and their IoNanofluids", *J. Phys. Chem. B*, to be submitted] are on the left (pure and with MWCNTs) and NEMD values on the right (pure, with SWCNT and with Graphene). "MP 350" stands for the Müller-Plathe method with a kinetic energy exchange rate of 350 time steps, while "MP 500" stands for a kinetic energy exchange rate of 500 time steps.

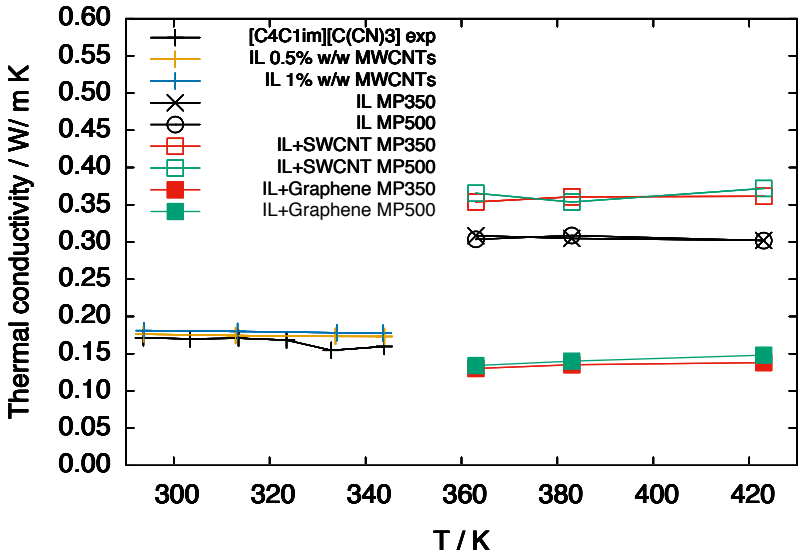


Figure S20. Thermal conductivity of $[C_4C_1im][C(CN)_3]$, pure and with carbon nanomaterials. Experimental results [J.M.P. França, S.M.S. Murshed, A.A.H Pádua, C.A. Nieto de Castro, "Thermal conductivity of Cyano and Phosphonium Ionic Liquids and their IoNanofluids", *J. Phys. Chem. B*, to be submitted] are on the left (pure and with MWCNTs) and NEMD values on the right (pure, with SWCNT and with Graphene). "MP 350" stands for the Müller-Plathe method with a kinetic energy exchange rate of 350 time steps, while "MP 500" stands for a kinetic energy exchange rate of 500 time steps.

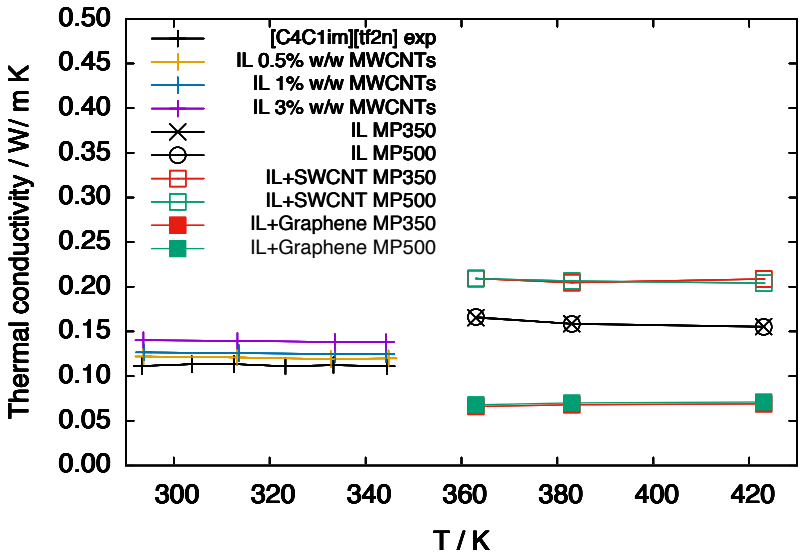


Figure S21. Thermal conductivity of $[C_4C_1im][tf_2N]$, pure and with carbon nanomaterials. Experimental results [J.M.P. França, *et al.*, *J. Chem. Eng. Data*, 2013, **58**, 467-476] are on the left (pure and with MWCNTs) and NEMD values on the right (pure, with SWCNT and with Graphene). "MP 350" stands for the Müller-Plathe method with a kinetic energy exchange rate of 350 time steps, while "MP 500" stands for a kinetic energy exchange rate of 500 time steps.

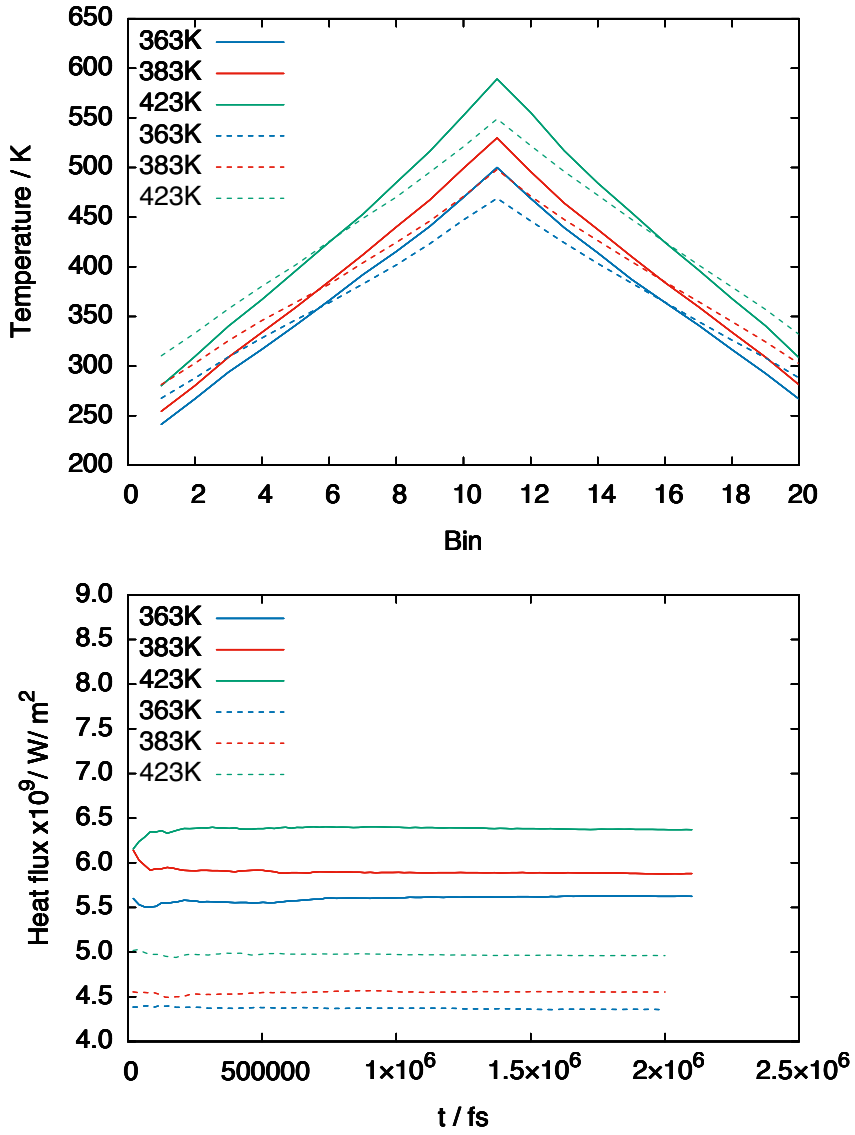


Figure S22. Temperature profile along the simulation box (here represented in bins) (top) and heat flux (bottom) for pure [$C_4C_1$im][SCN]. Solid lines represent a 350 time steps exchange rate of kinetic energy and the dashed lines represent 500 time steps exchange rate of kinetic energy.

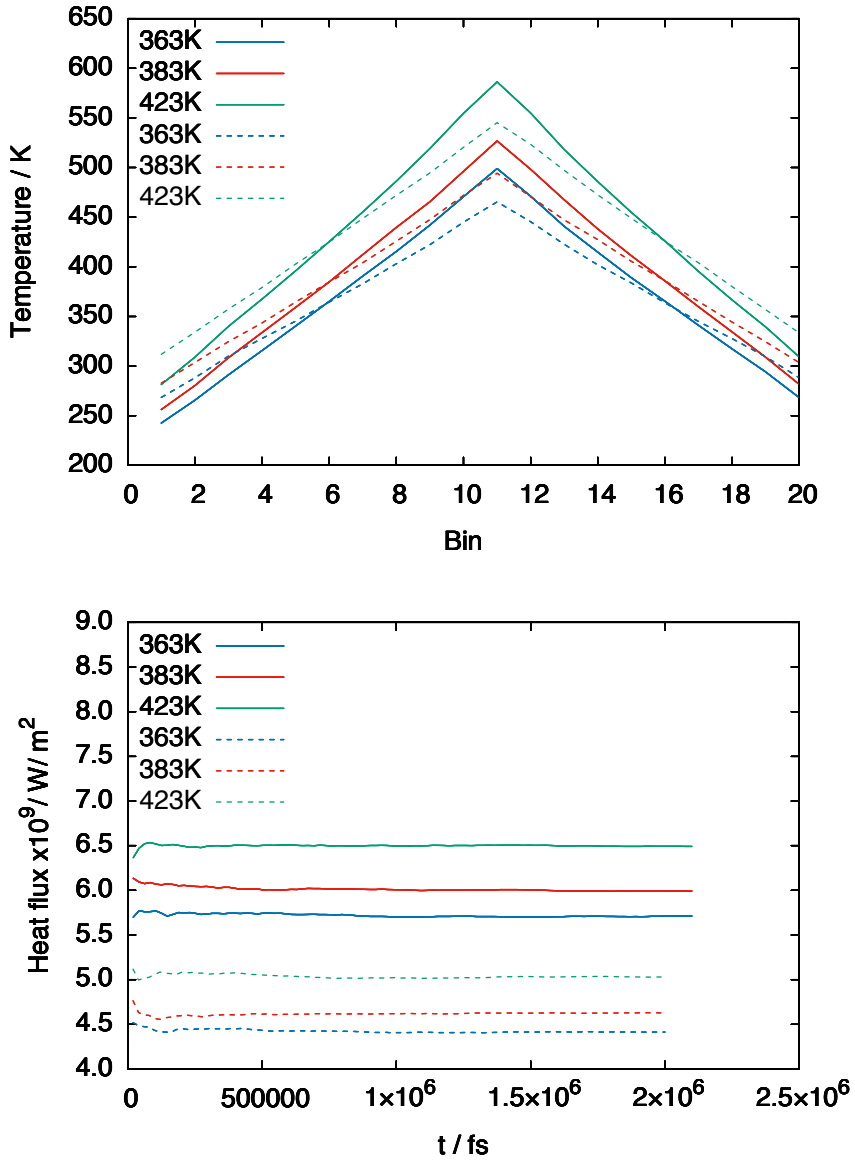


Figure S23. Temperature profile along the simulation box (here represented in bins) (top) and heat flux (bottom) for pure $[C_4C_1im][N(CN)_2]$. Solid lines represent a 350 time steps exchange rate of kinetic energy and the dashed lines represent 500 time steps exchange rate of kinetic energy.

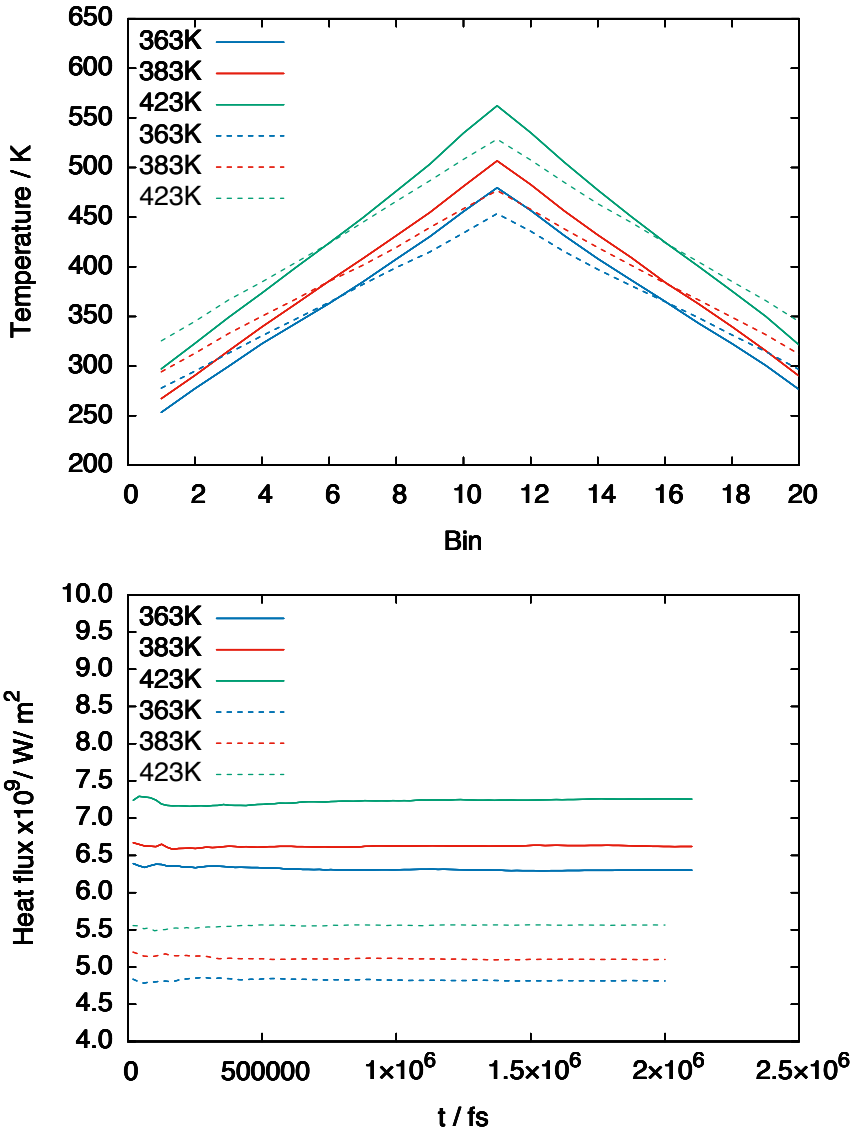


Figure S24. Temperature profile along the simulation box (here represented in bins) (top) and heat flux (bottom) for pure $[C_4C_1im][C(CN)_3]$. Solid lines represent a 350 time steps exchange rate of kinetic energy and the dashed lines represent 500 time steps exchange rate of kinetic energy.

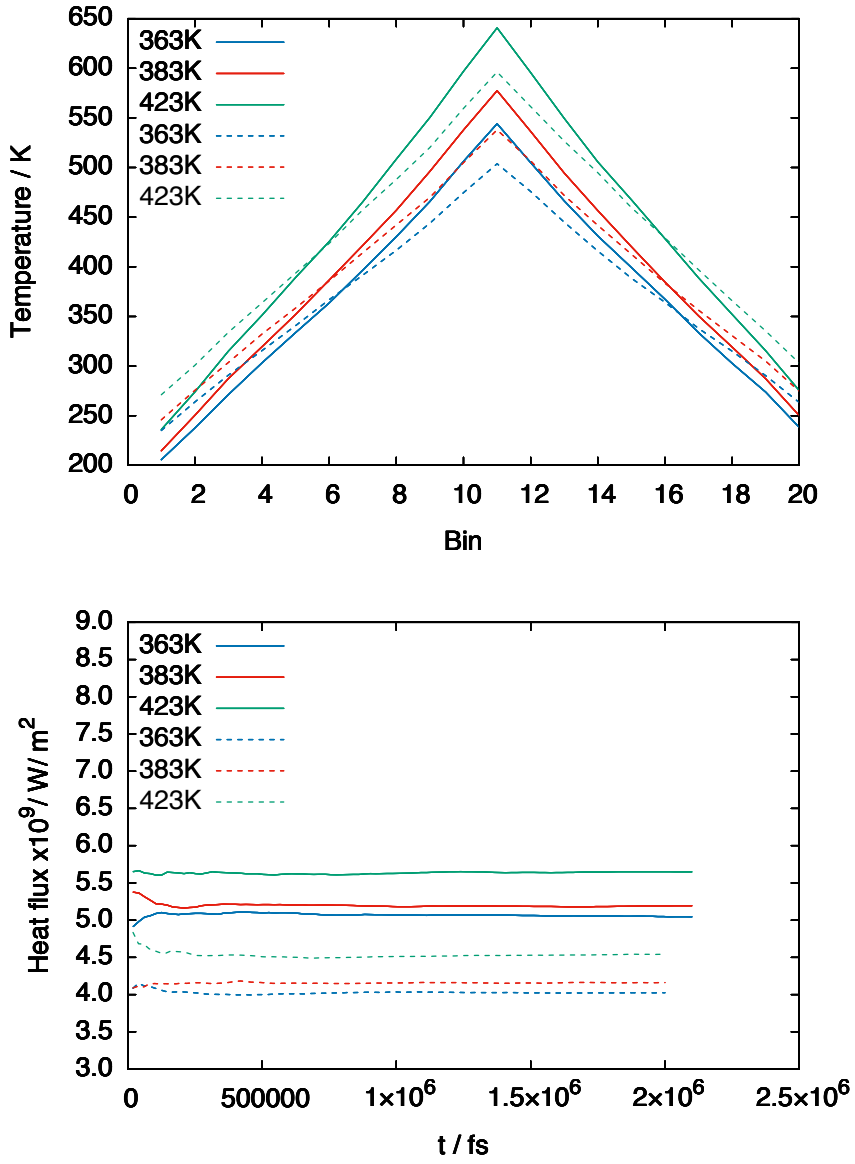


Figure S25. Temperature profile along the simulation box (here represented in bins) (top) and heat flux (bottom) for pure $[C_4C_1im][tf_2N]$. Solid lines represent a 350 time steps exchange rate of kinetic energy and the dashed lines represent 500 time steps exchange rate of kinetic energy.

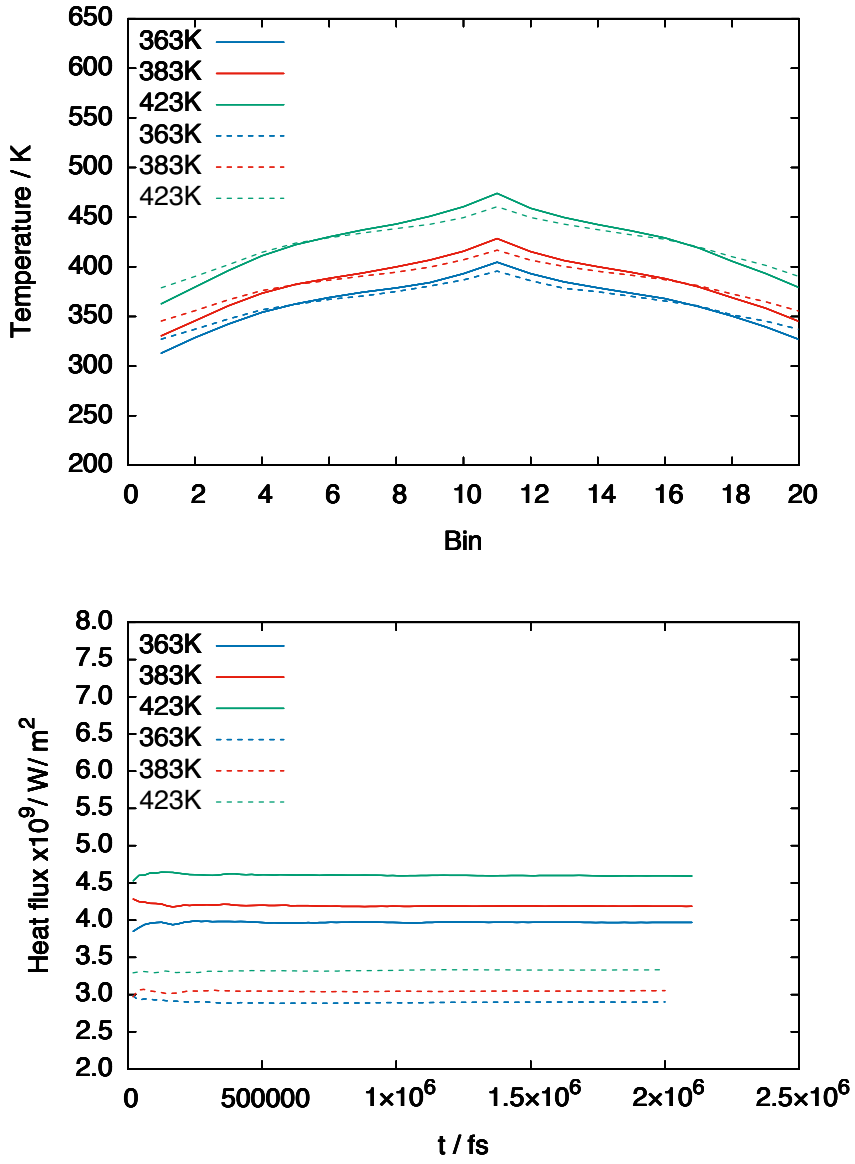


Figure S26. Temperature profile along the simulation box (here represented in bins) (top) and heat flux (bottom) for $[C_4C_1im][SCN]$ + SWCNT. Solid lines represent a 350 time steps exchange rate of kinetic energy and the dashed lines represent 500 time steps exchange rate of kinetic energy.

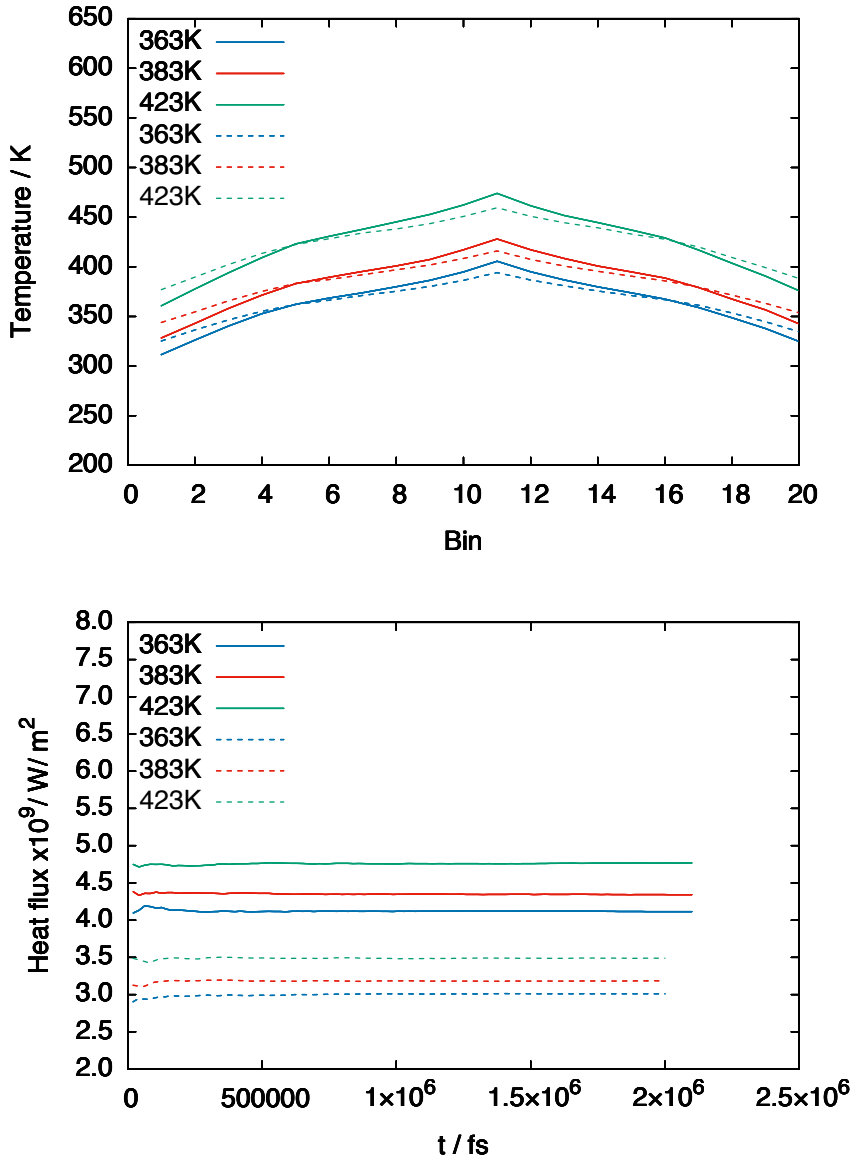


Figure S27. Temperature profile along the simulation box (here represented in bins) (top) and heat flux (bottom) for $[C_4C_1im][N(CN)_2]$ + SWCNT. Solid lines represent a 350 time steps exchange rate of kinetic energy and the dashed lines represent 500 time steps exchange rate of kinetic energy.

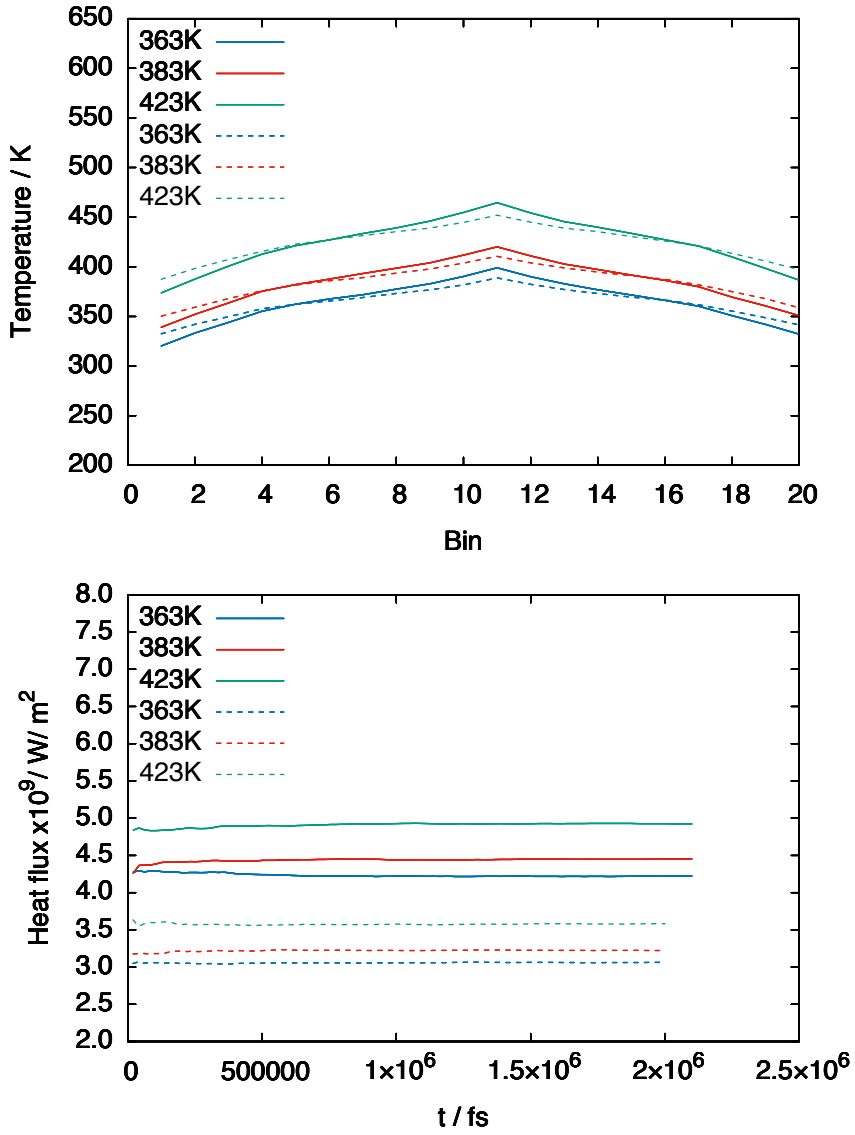


Figure S28. Temperature profile along the simulation box (here represented in bins) (top) and heat flux (bottom) for $[C_4C_1im][C(CN)_3]$ + SWCNT. Solid lines represent a 350 time steps exchange rate of kinetic energy and the dashed lines represent 500 time steps exchange rate of kinetic energy.

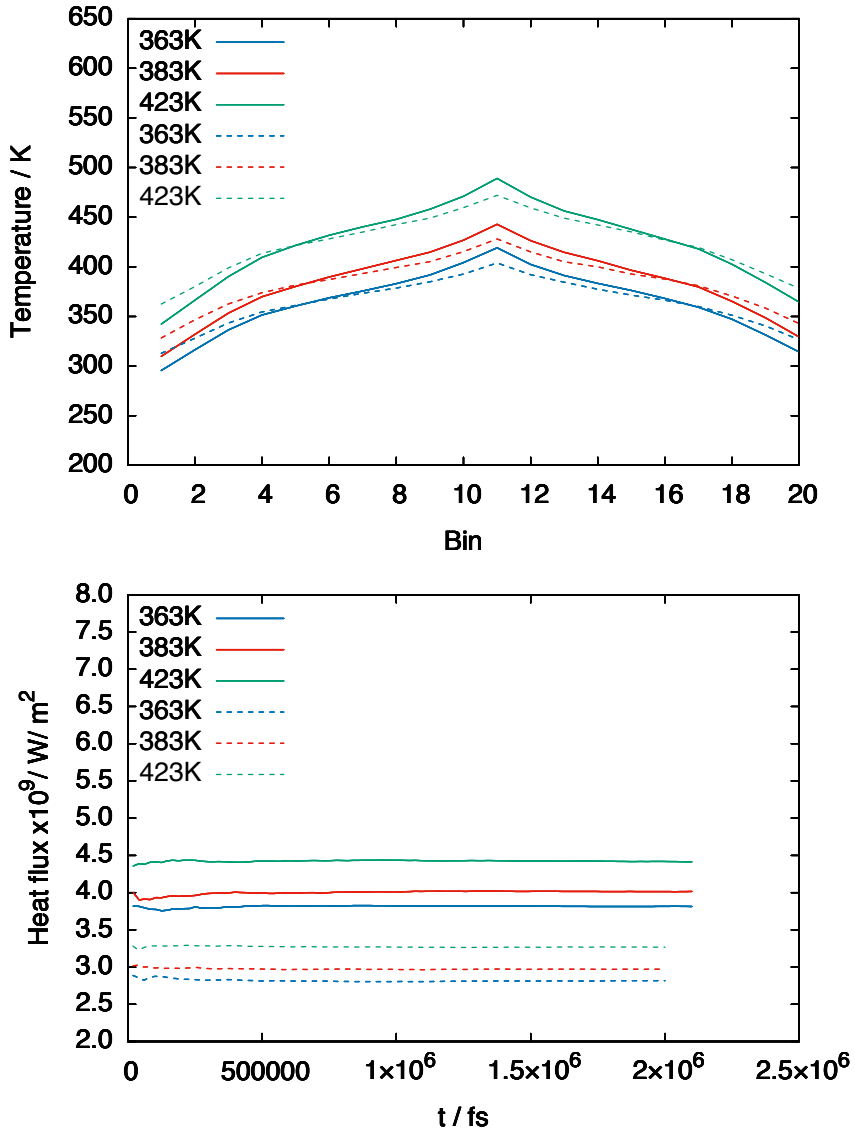


Figure S29. Temperature profile along the simulation box (here represented in bins) (top) and heat flux (bottom) for $[C_4C_1im][tf_2N]$ + SWCNT. Solid lines represent a 350 time steps exchange rate of kinetic energy and the dashed lines represent 500 time steps exchange rate of kinetic energy.

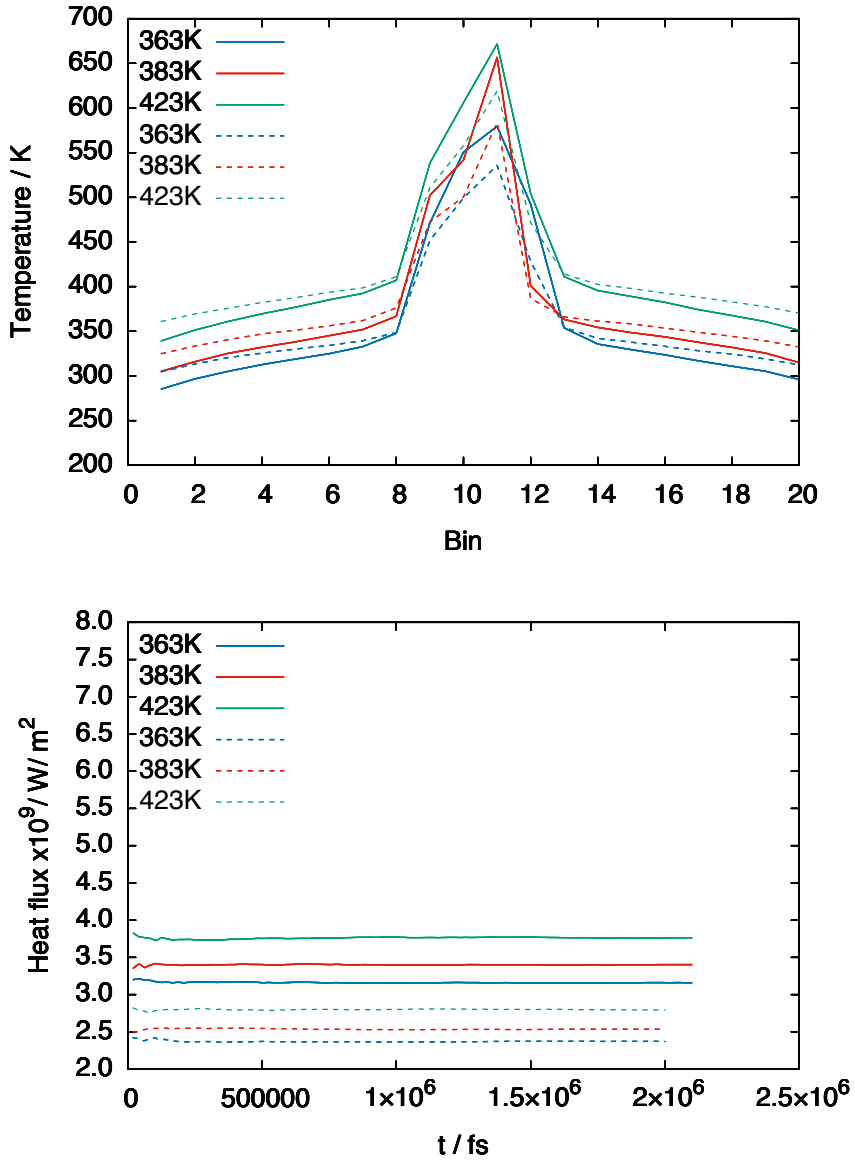


Figure S30. Temperature profile along the simulation box (here represented in bins) (top) and heat flux (bottom) for $[C_4C_1im][SCN]$ + Graphene. Solid lines represent a 350 time steps exchange rate of kinetic energy and the dashed lines represent 500 time steps exchange rate of kinetic energy.

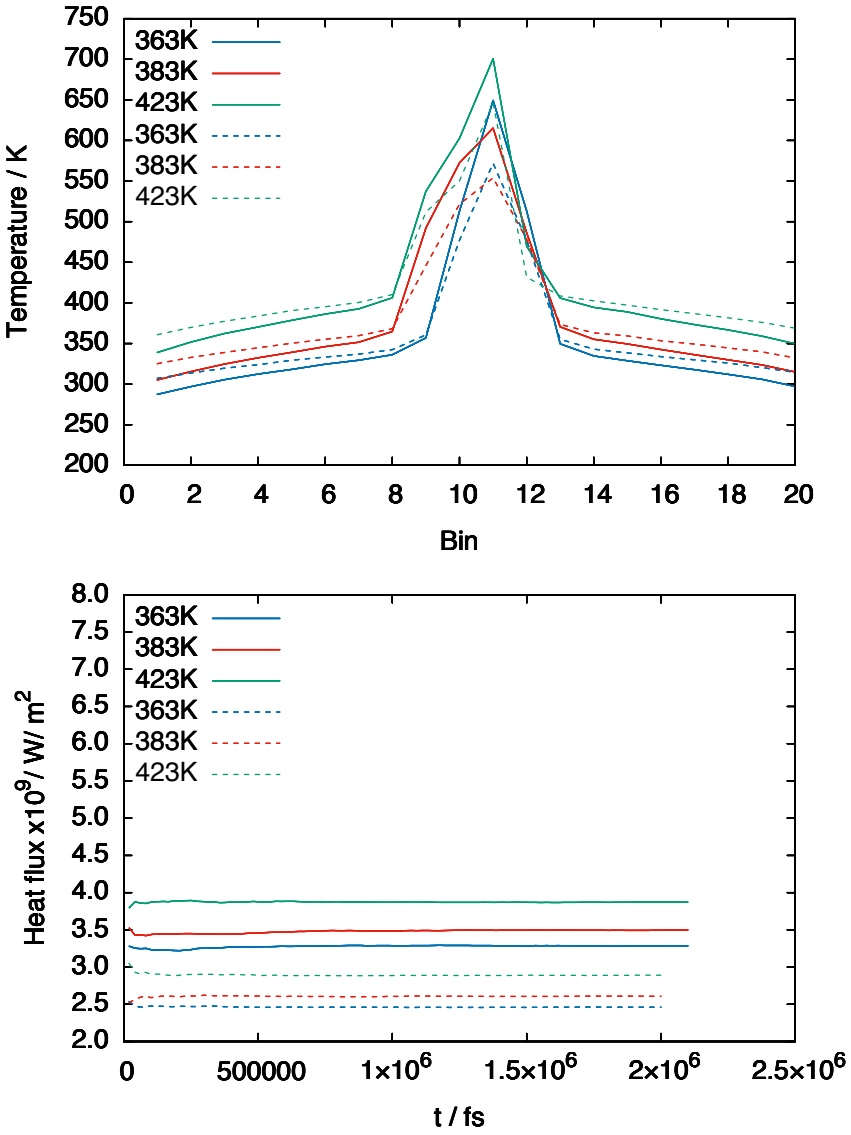


Figure S31. Temperature profile along the simulation box (here represented in bins) (top) and heat flux (bottom) for $[C_4C_1im][N(CN)_2]$ + Graphene. Solid lines represent a 350 time steps exchange rate of kinetic energy and the dashed lines represent 500 time steps exchange rate of kinetic energy.

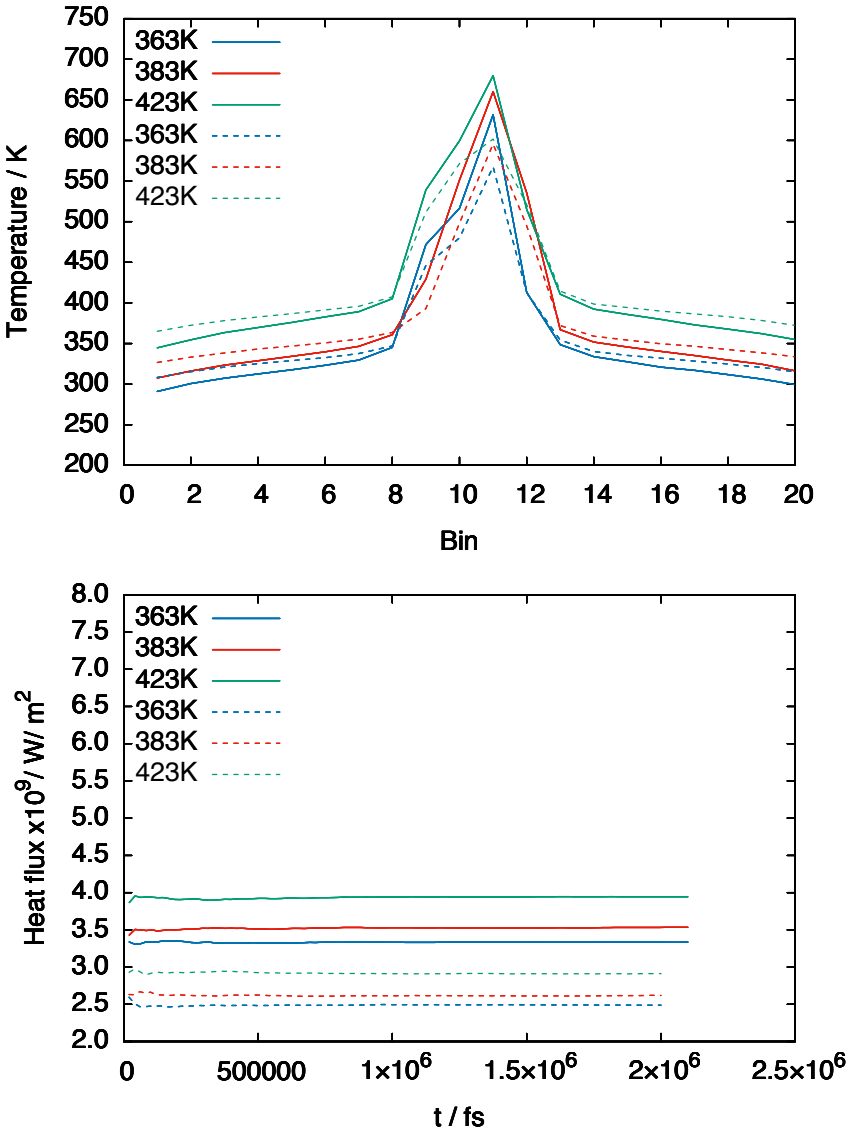


Figure S32. Temperature profile along the simulation box (here represented in bins) (top) and heat flux (bottom) for $[C_4C_1im][C(CN)_3]$ + Graphene. Solid lines represent a 350 time steps exchange rate of kinetic energy and the dashed lines represent 500 time steps exchange rate of kinetic energy.

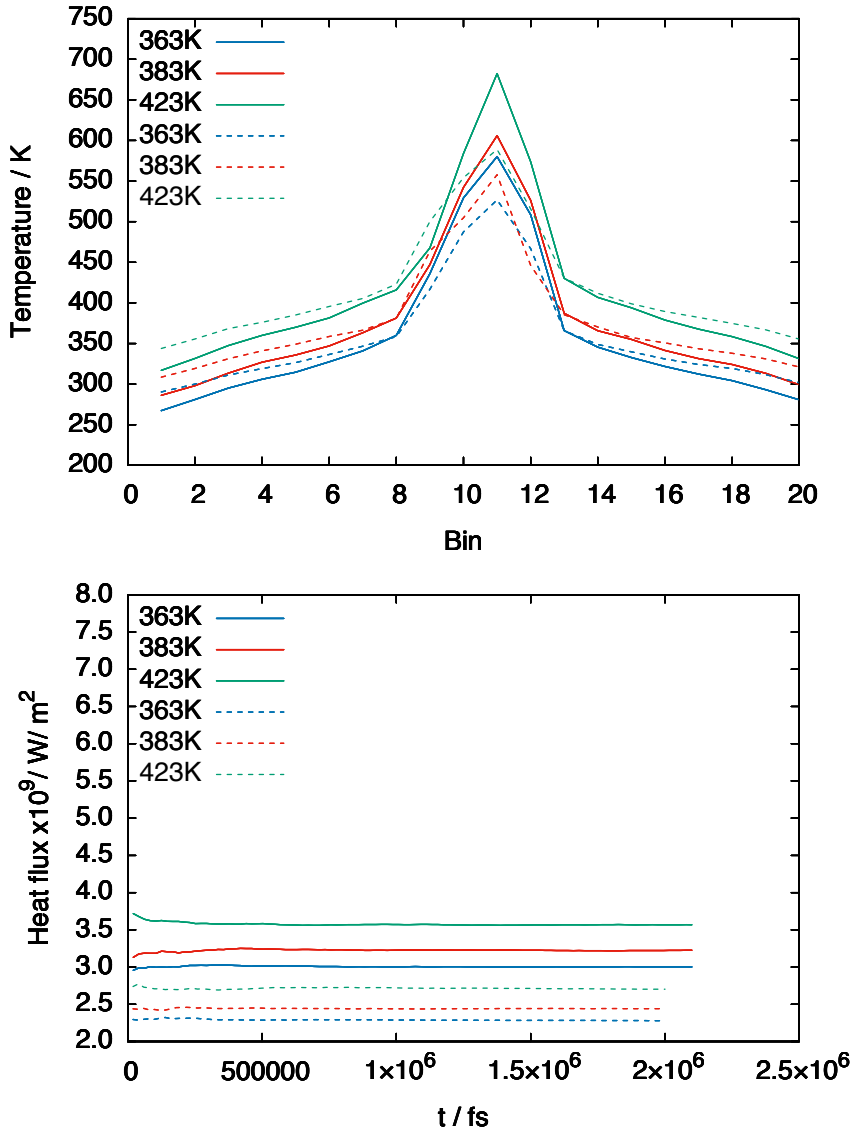


Figure S33. Temperature profile along the simulation box (here represented in bins) (top) and heat flux (bottom) for $[C_4C_1im][tf_2N]$ + Graphene. Solid lines represent a 350 time steps exchange rate of kinetic energy and the dashed lines represent 500 time steps exchange rate of kinetic energy.

Table S5. Comparison of thermal conductivity values obtained from NEMD for $[C_4C_1im][N(CN)_2]$ with SWCNT and graphene using different interaction potentials at 363 K. Kinetic energy exchanged once every 350 time steps.

| Potential | *n-m* | LJ |
|---|---|---|
| SWCNT | | |
| $\lambda$ / (W m$^{-1}$K$^{-1}$) IL | 0.253 | |
| $\lambda$ / (W m$^{-1}$K$^{-1}$) IL+SWCNT | 0.312 | 0.259 |
| Enhancement in $\lambda$ / % | 23.3 | 2.4 |
| Graphene | | |
| $\lambda$ / (W m$^{-1}$K$^{-1}$) IL bulk | 0.143 | 0.161 |
| $\lambda$ / (W m$^{-1}$K$^{-1}$) IL+Graphene | 0.127 | 0.131 |
| $\lambda$ / (W m$^{-1}$K$^{-1}$) interface | 0.188 | 0.184 |
| Enhancement $\lambda$ interface / % | 31.5 | 14.8 |

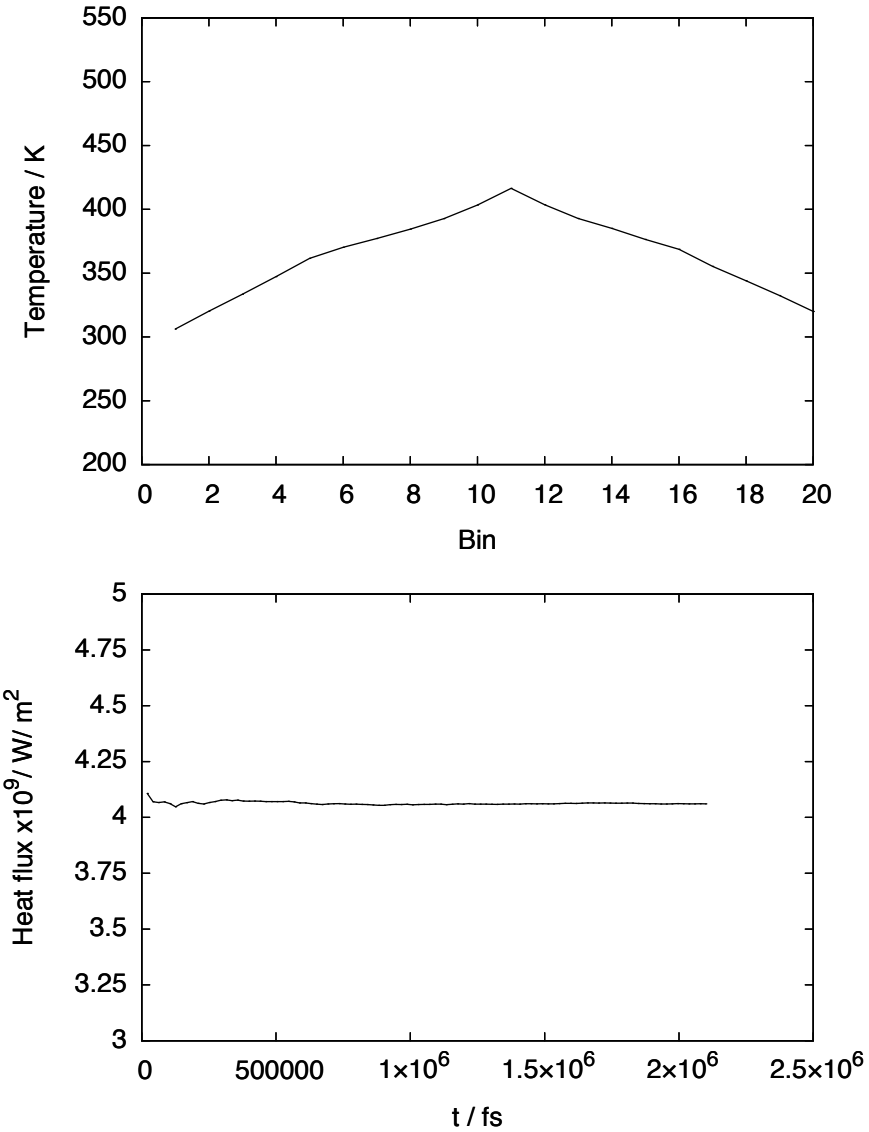


Figure S34. Temperature profile along the simulation box (here represented in bins) (top) and heat flux (bottom) for $[C_4C_1im][N(CN)_2]$ + SWCNT using a LJ potential with interaction parameters between ions and nanomaterial combination rules. Kinetic energy was exchanged once every 350 time steps.

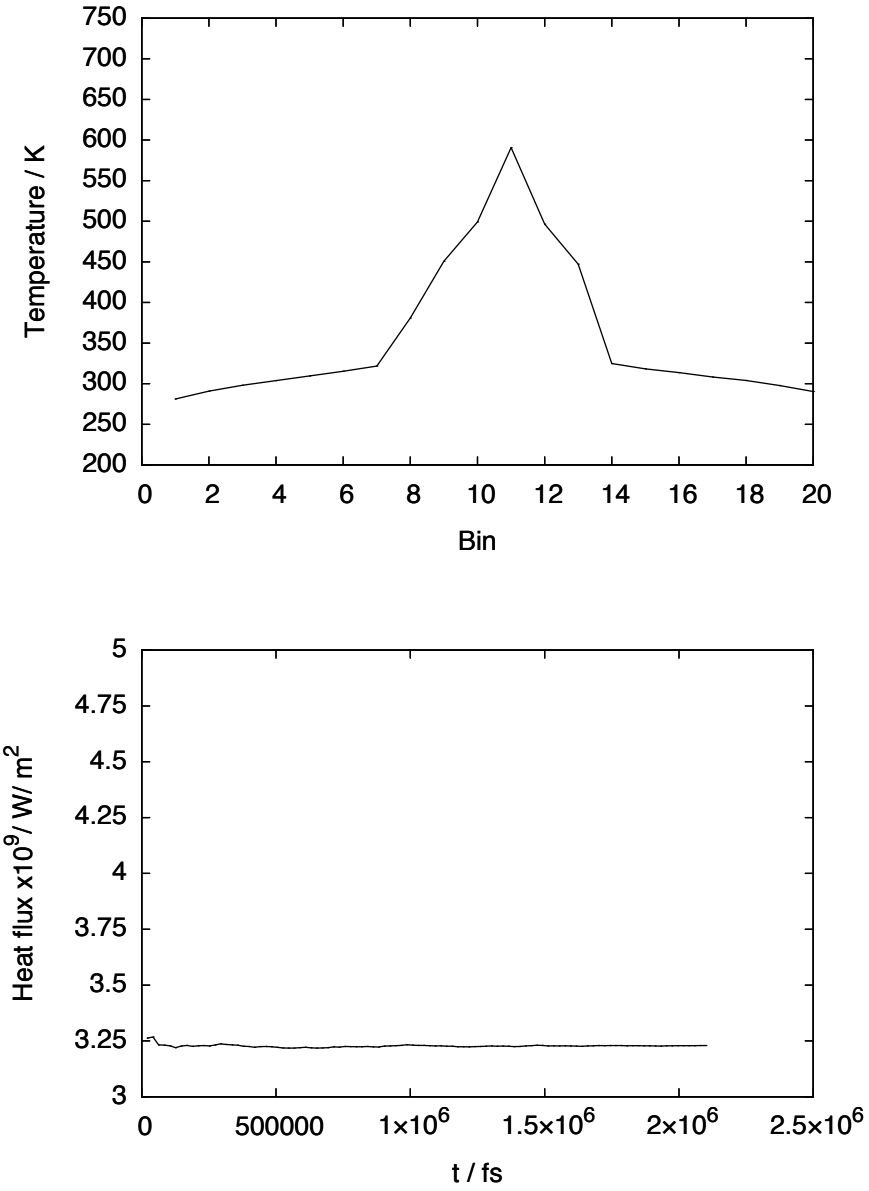


Figure S35. Temperature profile along the simulation box (here represented in bins) (top) and heat flux (bottom) for $[C_4C_1im][N(CN)_2]$ + Graphene using a LJ potential with interaction parameters between ions and nanomaterial combination rules. Kinetic energy was exchanged once every 350 time steps.